

*Reviewer 1# Remarks to the Author*

1. The text on 63-70 would likely lead a casual reader to think that your work was the first to use high-frequency measurements of isotopes in soil gas profiles, but this is not the case. I made a previous comment (not addressed in the response) about the importance of mentioning recent studies that have similarly worked with high-frequency measurements of C and O isotopes in soil profiles, using different analytical techniques. For example, the papers by Jochheim et al. 2018 (10.1002/jpln.201700259), and Bowling et al. 2015 (doi:10.5194/bg-12-5143-2015) are directly related to your topic and should be acknowledged. Also perhaps see Stumpp et al. 2018 (doi:10.2136/vzj2018.05.0096) and papers in that issue.

Response: First of all, we thank the reviewer for suggesting some relevant work done in this direction. We have referenced those studies in the modified version of our manuscript. We agree on the fact that several studies are already in place using high-frequency measurements of isotopes in soil gas profiles, and is not well addressed in our manuscript. However, we did not come across any work detailing simultaneous measurement of  $^{18}\text{O}$  and  $^{13}\text{C}$  in soil derived  $\text{CO}_2$  using an OA-ICOS, across a depth profile of 0 – 80cm. We consider our work to be novel in this aspect.

**“ Recently, several high frequency online measurements of  $\delta^{13}\text{C}$  and  $\delta^{18}\text{O}$  of soil  $\text{CO}_2$  and  $^2\text{H}$ ,  $^{18}\text{O}$  of soil water vapor across soil depth profiles were reported by coupling either hydrophobic but gas permeable membranes (installed at different depths in soil) or automated chamber systems with laser spectrometers (Bowling et al., 2015; Jochheim et al., 2018; Stumpp et al., 2018). Such approaches enable detection of vertical concentration profiles, temporal dynamics of soil  $\text{CO}_2$  concentration and isotopic signature of soil  $\text{CO}_2$  across different soil layers, thus aiding to identify and quantify various sources of  $\text{CO}_2$  across the depth profile.”**

2. I also previously made a comment with respect the “1 hz sampling frequency” that was not understood: “Finally, it should be noted that the useful temporal resolution of the measurements will never actually be 1hz as reported given the Allan variance results.” The point here, shown in Figure 3, is that the practical resolution of the measurement cannot be 1 hz because of the high variance in the measured delta values (especially for  $^{18}\text{O}$ , ~1.3 per mil) when estimated using 1 hz data. If we assume that precision of say ~0.1 - 0.2 per mil is adequate (obviously, this would depend on the specific study), the

useful sampling frequency would be ~10 – 20 seconds (0.05 – 0.1 hz). In fact, your in-situ soil measurements were conducted over 6 minute intervals to allow establishment of steady-state conditions. Please clarify accordingly in the Abstract. This detail is important for readers considering other applications of the method that might demand a higher sampling frequency.

Response: We agree with the reviewer on the fact that at better precision is not achieved at 1hz temporal resolution and that this is clear from the Allan variance results. This was a misunderstanding and is corrected in the manuscript.

“We established a real-time method for measuring soil CO<sub>2</sub> concentration,  $\delta^{13}\text{C}$  and  $\delta^{18}\text{O}$  values across a soil profile at higher temporal resolutions (0.05 – 0.1 hz) using an Off-Axis Integrated Cavity Output Spectrometer (OA-ICOS).”

### *Specific Comments*

1. 30-31: This statement is a truism, as atmospheric CO<sub>2</sub> will always diffuse into soil. What is relevant is the degree to which atmospheric CO<sub>2</sub> is diluted by soil-respired CO<sub>2</sub>. There is abundant previous work in this area. Please rephrase.

Response: We agree that such a rephrased in the modified manuscript.

“ $^{13}\text{C}$ -CO<sub>2</sub> of top soil at the calcareous soil site was found to be reflecting  $\delta^{13}\text{C}$  values of atmospheric CO<sub>2</sub> and  $\delta^{13}\text{C}$  of top soil CO<sub>2</sub> at the acidic soil site was representative of the biological respiratory processes.”

2. 31: What is the corollary—were  $^{18}\text{O}$  values decoupled from soil water at the calcareous site?

Response: At 80 cm depth in calcareous soil, the  $^{18}\text{O}$  values were found to be rather enriched relative to the upper soil layers. We rephrased the sentence as follows:

“ $\delta^{18}\text{O}$  values of CO<sub>2</sub> in both sites reflected the  $\delta^{18}\text{O}$  of soil water across most of the depth profile, except for the 80 cm depth at the calcareous site where a relative enrichment in  $^{18}\text{O}$  was observed.”

3. 38: “accurate monitoring and modeling of these fluxes are inevitable” I think you mean essential here, rather than inevitable?

Response: Yes, inevitable seems to be too strong for a word in this context. Corrected in the manuscript.

“To understand the prevailing climatic conditions and predict climate change, accurate monitoring and modeling of these fluxes are **essential** (Barthel et al., 2014; Harwood et al., 1999; Schär et al., 2004).”

4. 38: “Approximately 30 - 35% ...” note that the anthropogenic CO<sub>2</sub> flux has doubled since this paper was written so this statement is no longer correct.

Response: Agree. This is rectified in the modified manuscript.

**“Soil respiration, the CO<sub>2</sub> flux released from soil surface to the atmosphere as a result of microbial and root respiration (heterotrophic and autotrophic) is the second largest terrestrial carbon flux (Bond-Lamberty and Thomson, 2010).”**

5. 233: replace “inevitable” with “necessary” (that seems to be what you mean?)

Response: Yes, and is changed in the manuscript.

“we found that routine calibration (Correction for concentration-dependent error plus three-point calibration) was **necessary** for obtaining the required accuracy, in particular under fluctuating CO<sub>2</sub> concentrations.”

6. 270-277: There is a subtle misinterpretation of your carbonate end member <sup>13</sup>C values. It is stated “According to Cerling (1984), the distinct oxygen and carbon isotopic composition of soil carbonate depends on the isotopic signature of meteoric water and to the proportion of C<sub>4</sub> biomass present at the time of carbonate formation (Cerling, 1984).” Note that pedogenic carbonate <sup>13</sup>C reflects the <sup>13</sup>C of the CO<sub>2</sub> source of that carbonate (after accounting for fractionation), which is not simply a function of C<sub>3</sub> vs. C<sub>4</sub> biomass, but rather all of the other myriad factors that determine the <sup>13</sup>C value of soil CO<sub>2</sub>. This should be clarified. Then it is stated “CO<sub>2</sub> released as a result from carbonates have a distinct δ<sup>13</sup>C value close to 0‰ vs. VPDB.” Really, the CO<sub>2</sub> released from carbonate will have whatever <sup>13</sup>C value the carbonate had to begin with (assuming complete conversion through bicarbonate to CO<sub>2</sub>, without fractionation). Note that these in fact have <sup>13</sup>C values much lower than zero per mil at your site! You have now measured carbonate <sup>13</sup>C so you can be more precise here.

Response: Agree, as it is clear from our carbonate  $^{13}\text{C}$  measurements, the major proportion of carbonate in our study site (calcareous) is pedogenic. However, the  $^{13}\text{C}$  signal of  $\text{CO}_2$  emanating from geogenic carbonates will have an isotopic signal close to 0‰ vs. VPDB. From our carbonate  $^{13}\text{C}$  analysis, we get to see that  $^{13}\text{C}$  signal is approximately close to -6‰ at 80 cm depth and near -9‰ at the upper layers. Since soil at the calcareous site is fluvic Gleysol, the possibility of geogenic carbonates contributing to the  $^{13}\text{C}$ - $\text{CO}_2$  signature cannot be neglected. Hence it is probably a mix of biogenic, pedogenic and geogenic carbonates that contribute to the observed  $^{13}\text{C}$  signature.

“According to Cerling (1984), the distinct oxygen and carbon isotopic composition of soil carbonate depends primarily on the isotopic signature of meteoric water and to the proportion of  $\text{C}_4$  biomass present at the time of carbonate formation (Cerling, 1984), but also on numerous other factors that determine the  $^{13}\text{C}$  value of soil  $\text{CO}_2$ .  $\text{CO}_2$  released as a result from carbonates in calcareous soil site have a distinct  $\delta^{13}\text{C}$  value of -9.3 (mean value across soil profile 0 - 80 cm depth) (Figure 8(c)), while  $\text{CO}_2$  released during biological respiratory processes has  $\delta^{13}\text{C}$  values around -24‰ as observed in the acidic soil (Figure 10 (e)). The  $\delta^{13}\text{C}$  values of soil  $\text{CO}_2$  observed in the deepest soil layer in the calcareous soil site most likely indicates the presence of carbonate sources of pedogenic and geologic origin.”

7. 283: You measured total inorganic C, not bicarbonate, correct? Is this a typo or something else?

Response: We have measured total Carbon content (that include both organic and inorganic carbon), bulk soil  $\delta^{13}\text{C}$ , carbonate  $\delta^{13}\text{C}$  &  $\delta^{18}\text{O}$  values. For measuring carbonate  $\delta^{13}\text{C}$  &  $\delta^{18}\text{O}$  values We extracted  $\text{CO}_2$  from carbonate by treating with phosphoric acid (for details see <https://doi.org/10.1016/j.ijms.2006.11.006>)

8. 291: Also organic acids (or any other source of  $\text{H}^+$ ), which are perhaps most important. Note that acidity generated from  $\text{CO}_2$  (carbonic acid) will dissolve carbonate to form bicarbonate, but this is a net zero  $\text{CO}_2$  flux, even though you will observe the  $^{13}\text{C}$  from the carbonate due to exchange. See for example Zamanian et al. 2016, <http://dx.doi.org/10.1016/j.earscirev.2016.03.003>

Response: Thanks for the reference, This relevant information is added in the modified manuscript.

“Water content, soil CO<sub>2</sub> concentration and presence of organic acids or any other source of H<sup>+</sup> are the major factors influencing carbonate weathering, and variations in soil CO<sub>2</sub> partial pressure, moisture, temperature, and pH can cause degassing of CO<sub>2</sub> which contributes to the soil CO<sub>2</sub> efflux (Schindlbacher et al., 2015; Zamanian et al., 2016). CaCO<sub>3</sub> solubility in pure H<sub>2</sub>O at 25°C is 0.013 gL<sup>-1</sup>, but in weak acids like carbonic acid, the solubility is increased up to five fold (Zamanian et al., 2016). The production of carbonic acid due to CO<sub>2</sub> dissolution will convert carbonate to bicarbonates resulting in exchange of carbon atoms between carbonates and dissolved CO<sub>2</sub>.”

9. 328-329: This is another place where relevant recent studies of soil gas isotope dynamics should be cited.

Response: Recent studies of soil gas isotope dynamics are now cited in the modified manuscript.

“Given the fact that laser-based CO<sub>2</sub> isotope analyzers are deployed on site in combination with different gas sampling methods like automated chambers systems (Bowling et al., 2015), and hydrophobic gas permeable membranes (Jochheim et al., 2018) for tracing various ecosystem processes, it is important to address this issue.”

10. Figure 6: What do the colored dashed lines represent? There is no indication in the legend. Are they some kind of error around the solid colored lines?

Response: Colored dashed lines denote 95% confidence interval. This is corrected in the manuscript.

11. Figure 7: What CO<sub>2</sub> mole fractions were used to generate this figure? This seems important in light of Figure 6

Response:  $\delta^{13}\text{C}$  and  $\delta^{18}\text{O}$  values corresponding to CO<sub>2</sub> concentrations ranging from 400 ppm to 25000 ppm are used to generate the 3-point calibration lines.

3 **Application of a laser-based spectrometer for continuous insitu**  
4 **measurements of stable isotopes of soil CO<sub>2</sub> in calcareous and**  
5 **acidic soils**

6 J. Joseph<sup>1</sup>, C. Külls<sup>2</sup>, M. Arend<sup>3</sup>, M. Schaub<sup>1</sup>, F. Hagedorn<sup>1</sup>, A. Gessler<sup>1</sup> and M. Weiler<sup>4</sup>

7 [1] {Swiss Federal Institute for Forest, Snow and Landscape Research WSL, Zürcherstrasse 111, 8903  
8 Birmensdorf, Switzerland}

9 [2] {Laboratory for Hydrology and International Water Management, University of Applied Sciences Lübeck,  
10 Germany}

11 [3] {Physiological Plant Ecology (PPE), Faculty of Integrative Biology, University of Basel, Switzerland}

12 [4] {Chair of Hydrology, Faculty of Environment and Natural resources, University of Freiburg, Germany}

13 Correspondence to: J. Joseph (jobin.joseph@wsl.ch)

14

15

16 **Abstract**

17 The short-term dynamics of carbon and water fluxes across the soil-plant-atmosphere continuum are still not fully  
18 understood. One important constraint is the lack of methodologies that enable simultaneous measurements of soil  
19 CO<sub>2</sub> concentration and respective isotopic composition at a high temporal resolution for longer periods of time.  
20 δ<sup>13</sup>C of soil CO<sub>2</sub> can be used to derive information on the origin and physiological history of carbon and δ<sup>18</sup>O in  
21 soil CO<sub>2</sub> aids to infer interaction between CO<sub>2</sub> and soil water. We established a real-time method for measuring  
22 soil CO<sub>2</sub> concentration, δ<sup>13</sup>C and δ<sup>18</sup>O values across a soil profile at higher temporal resolutions (0.05 – 0.1 hz)  
23 using an Off-Axis Integrated Cavity Output Spectrometer (OA-ICOS). We also developed a calibration method  
24 correcting for the sensitivity of the device against concentration-dependent shifts in δ<sup>13</sup>C and δ<sup>18</sup>O values under  
25 highly varying CO<sub>2</sub> concentration. The deviations of measured data were modelled, and a mathematical correction  
26 model was developed and applied for correcting the shift. By coupling an OA-ICOS with hydrophobic but gas  
27 permeable membranes placed at different depths in acidic and calcareous soils, we investigated the contribution of  
28 abiotic and biotic components to total soil CO<sub>2</sub> release. We found that in the calcareous Gleysol, CO<sub>2</sub> originating  
29 from carbonate dissolution contributed to the total soil CO<sub>2</sub> concentration at detectable degrees potentially due to  
30 CO<sub>2</sub> evasion from groundwater. <sup>13</sup>C-CO<sub>2</sub> of top soil at the calcareous soil site was found to be reflecting δ<sup>13</sup>C  
31 values of atmospheric CO<sub>2</sub> and δ<sup>13</sup>C of top soil CO<sub>2</sub> at the acidic soil site was representative of the biological  
32 respiratory processes. δ<sup>18</sup>O values of CO<sub>2</sub> in both sites reflected the δ<sup>18</sup>O of soil water across most of the depth  
33 profile, except for a relative enrichment in <sup>18</sup>O was observed at 80 cm depth at the calcareous site .

34

35 **Key words:** δ<sup>13</sup>C, δ<sup>18</sup>O, OA-ICOS, hydrophobic/gas permeable membrane.

36

## 37 1 Introduction

38 Global fluxes of CO<sub>2</sub> and H<sub>2</sub>O are two major driving forces controlling earth's climatic systems. To understand the  
39 prevailing climatic conditions and predict climate change, accurate monitoring and modeling of these fluxes are  
40 essential (Barthel et al., 2014; Harwood et al., 1999; Schär et al., 2004). Soil respiration, the CO<sub>2</sub> flux released  
41 from soil surface to the atmosphere as a result of microbial and root respiration (heterotrophic and autotrophic) is  
42 the second largest terrestrial carbon flux (Bond-Lamberty and Thomson, 2010). The long-term dynamics of CO<sub>2</sub>  
43 release on a seasonal scale are reasonably well understood (Satakhun et al., 2013), whereas less information on  
44 CO<sub>2</sub> dynamics and isotopic composition are available for short-term variations on a diurnal scale (Werner and  
45 Gessler, 2011). The lack of proper understanding of the diurnal fluctuations in soil CO<sub>2</sub> release might introduce  
46 uncertainty in estimating the soil carbon budget and the CO<sub>2</sub> fluxes to the atmosphere. The isotopic composition  
47 of soil CO<sub>2</sub> and its diel fluctuation can be a critical parameter for the partitioning of ecosystem gas exchange into  
48 its components (Bowling et al., 2003; Mortazavi et al., 2004) and for disentangling plant and ecosystem processes  
49 (Werner and Gessler 2011). By assessing  $\delta^{13}\text{C}$  of soil CO<sub>2</sub>, it is possible to identify the source for CO<sub>2</sub> (Kuzyakov,  
50 2006) and the coupling between photosynthesis and soil respiration when taking into account post-photosynthetic  
51 isotope fractionation (Werner et al., 2012; Wingate et al., 2010).  $\delta^{13}\text{C}$  soil CO<sub>2</sub> reflects, however, not only microbial  
52 and root respiration but also abiotic sources from carbonate weathering (Schindlbacher et al., 2015).

53 Soil water imprints its  $\delta^{18}\text{O}$  signature on soil CO<sub>2</sub> as a result of isotope exchange between H<sub>2</sub>O and CO<sub>2</sub> (aqueous).  
54 The oxygen isotopic exchange between CO<sub>2</sub> and soil water is catalyzed by microbial carbonic anhydrase (Sperber  
55 et al., 2015; Wingate et al., 2009). Thus, soil CO<sub>2</sub> can give information on the isotopic composition of both soil  
56 water resources and carbon sources. The oxygen isotope composition of plant-derived CO<sub>2</sub> is both, a tracer of  
57 photosynthetic and respiratory CO<sub>2</sub> and gives additional quantitative information on the water cycle in terrestrial  
58 ecosystems (Francey and Tans, 1987). To better interpret the  $\delta^{13}\text{C}$  and  $\delta^{18}\text{O}$  signals of atmospheric CO<sub>2</sub>, the  
59 isotopic composition and its variability of the different sources need to be better understood (Werner et al., 2012;  
60 Wingate et al., 2010).

61 The conventional method to estimate  $\delta^{13}\text{C}$  and  $\delta^{18}\text{O}$  of soil CO<sub>2</sub> efflux is by using two end-member mixing models  
62 of atmospheric CO<sub>2</sub> and CO<sub>2</sub> produced in the soil (Keeling, 1958). The conventional methods for sampling soil  
63 produced CO<sub>2</sub> are chamber based (Bertolini et al., 2006; Torn et al., 2003), 'mini-tower' (Kayler et al., 2010;  
64 Mortazavi et al., 2004), and soil gas well (Breecker and Sharp, 2008; Oerter and Amundson, 2016) based methods.  
65 In conventional methods, air sampling is done at specific time intervals, and  $\delta^{13}\text{C}$  and  $\delta^{18}\text{O}$  are analyzed using  
66 Isotope Ratio Mass Spectrometry (IRMS) (Ohlsson et al., 2005). Such offline methods have several disadvantages  
67 like high sampling costs, excessive time consumption for sampling and analysis, increased sampling error and low  
68 temporal resolution. Kammer et al. (2011), showed how error-prone the conventional methods could be while  
69 calculating  $\delta^{13}\text{C}$  and  $\delta^{18}\text{O}$  (up to several per mil when using chamber and mini tower-based methods) (Kammer et  
70 al., 2011). In chamber-based systems, non-steady-state conditions may arise within the chamber due to increased  
71 CO<sub>2</sub> concentrations which in turn hinders the diffusion of <sup>12</sup>CO<sub>2</sub> more strongly than that of heavier <sup>13</sup>CO<sub>2</sub> (Risk  
72 and Kellman, 2008). Moreover, it has been found that  $\delta^{18}\text{O}$  of CO<sub>2</sub> inside a chamber is significantly influenced by  
73 the  $\delta^{18}\text{O}$  of the surface soil water as an equilibrium isotopic exchange happens during the upward diffusive  
74 movement of soil CO<sub>2</sub> (Mortazavi et al., 2004). The advent of laser-based isotope spectroscopy has enabled cost-  
75 effective, simple, and high precision real-time measurements of  $\delta^{13}\text{C}$  and  $\delta^{18}\text{O}$  in CO<sub>2</sub> (Kammer et al., 2011; Kerstel

76 and Gianfrani, 2008). This technique opened up new possibilities for faster and reliable measurements of stable  
77 isotopes insitu, based on the principle of light absorption, using laser beams of distinct wavelengths in the near and  
78 mid-infrared range (Bowling et al., 2003). Recently, several high frequency online measurements of  $\delta^{13}\text{C}$  and  $\delta^{18}\text{O}$   
79 of soil  $\text{CO}_2$  and  $^2\text{H}$ ,  $^{18}\text{O}$  of soil water vapor across soil depth profiles were reported by coupling either hydrophobic  
80 but gas permeable membranes (installed at different depths in soil) or automated chamber systems with laser  
81 spectrometers (Bowling et al., 2015; Jochheim et al., 2018; Stumpp et al., 2018). Such approaches enable detection  
82 of vertical concentration profiles, temporal dynamics of soil  $\text{CO}_2$  concentration and isotopic signature of soil  $\text{CO}_2$   
83 across different soil layers, thus aiding to identify and quantify various sources of  $\text{CO}_2$  across the depth profile.

84 In 1988, O'Keefe and Deacon introduced the Cavity Ring-Down Spectroscopy (CRDS) for measuring the isotopic  
85 ratio of different gaseous species based on laser spectrometry (O'Keefe and Deacon, 1988). With the laser-based  
86 spectrometry techniques, measuring sensitivities up to parts per trillion (ppt) concentrations are achieved (von  
87 Basum et al., 2004; Peltola et al., 2012). In CRDS, the rate of change in the absorbed radiation of laser light that  
88 is temporarily "trapped" within a highly reflective optical cavity is determined. This is achieved using resonant  
89 coupling of a laser beam to the optical cavity and active locking of laser frequency to cavity length (Parameswaran  
90 et al., 2009). Another well-established technique similar to CRDS is Off-Axis Integrated Cavity Output  
91 Spectroscopy (OA-ICOS). It is based on directing lasers with narrowband and continuous-wave in an off-axis  
92 configuration to the optical cavity (Baer et al., 2002).

93 Even though OA-ICOS can measure concentration and isotope signature of various gaseous species at high  
94 temporal resolution, we found pronounced deviations in  $\delta^{13}\text{C}$  and  $\delta^{18}\text{O}$  measurements from the absolute values  
95 when measured under changing  $\text{CO}_2$  concentrations. So far to our knowledge, no study has been made available  
96 detailing the calibration process of OA-ICOS  $\text{CO}_2$  analyzers correcting for fluctuations of both  $\delta^{13}\text{C}$  and  $\delta^{18}\text{O}$   
97 values under varying  $\text{CO}_2$  concentrations. Most of the OA-ICOS  $\text{CO}_2$  analyzers are built for working under stable  
98  $\text{CO}_2$  concentrations, so that periodical calibration against in-house gas standards at a particular concentration is  
99 sufficient. However, as there are pronounced gradients in  $\text{CO}_2$  levels in soils (Maier and Schack-Kirchner, 2014),  
100  $\text{CO}_2$  concentration depending shifts in measured isotopic values have to be addressed and corrected. Such  
101 calibration is, however, also relevant for any other OA-ICOS application with varying levels of  $\text{CO}_2$  (e.g., in  
102 chamber measurements). Hence the first part of this work comprises the establishment of a calibration method for  
103 OA-ICOS. The second part describes a method for online measurement of  $\text{CO}_2$  concentrations and stable carbon  
104 and oxygen isotope composition of  $\text{CO}_2$  in different soil depths by coupling OA-ICOS with gas permeable  
105 hydrophobic tubes (Membrane tubes, Accurel®). The use of these tubes for measuring soil  $\text{CO}_2$  concentration (Gut  
106 et al., 1998) and  $\delta^{13}\text{C}$  of soil  $\text{CO}_2$  (Parent et al., 2013) has already been established, but the coupling to an OA-  
107 ICOS system has not been performed, yet.

108 We evaluated our measurement system by assessing and comparing the concentration,  $\delta^{13}\text{C}$  and  $\delta^{18}\text{O}$  of soil  $\text{CO}_2$   
109 for a calcareous and an acidic soil system. The primary foci of this study are to (1) introduce OA-ICOS in online  
110 soil  $\text{CO}_2$  concentration and isotopic measurements; (2) calibrate the OA-ICOS to render it usable for isotopic  
111 analysis carried out under varying  $\text{CO}_2$  concentrations; and (3) analyze the dynamics of  $\delta^{13}\text{C}$  and  $\delta^{18}\text{O}$  of soil  $\text{CO}_2$   
112 at different soil depths in different soil types at a higher temporal resolution.

113

## 114 **2 Materials and Methods**

### 115 **2.1 Instrumentation**

116 The concentration,  $\delta^{13}\text{C}$  and  $\delta^{18}\text{O}$  values of  $\text{CO}_2$  were measured with an OA-ICOS, as described in detail by (Baer  
117 et al., 2002; Jost et al., 2006). In this study, we used an OA-ICOS, (LGR-CCIA 36-d) manufactured by Los Gatos  
118 Research Ltd, San-Francisco, USA. LGR-CCIA 36-d measures  $\text{CO}_2$  concentration, and  $\delta^{13}\text{C}$  and  $\delta^{18}\text{O}$  values at a  
119 frequency up to 1 Hz. The operational  $\text{CO}_2$  concentration range was 400 to 25,000 ppm. Operating temperature  
120 range was +10 - +35°C, and sample temperature range (Gas temperature) was between -20°C and 50°C.  
121 Recommended inlet pressure was < 0.0689 MPa. The multiport inlet unit, an optional design that comes along with  
122 LGR-CCIA 36-d, had a manifold of 8 digitally controlled inlet ports and one outlet port. It rendered the user with  
123 an option of measuring eight different  $\text{CO}_2$  samples at the desired time interval. Three standard gases with distinct  
124  $\delta^{13}\text{C}$  and  $\delta^{18}\text{O}$  values were used for calibration in this study (See Supplementary Table.1). The standard gases used  
125 in this study were analyzed for absolute concentration and respective  $\delta^{13}\text{C}$  and  $\delta^{18}\text{O}$  values.  $\delta$ -values are expressed  
126 based on Vienna Pee Dee Belemnite (VPDB)- $\text{CO}_2$  scale, and were determined by high precision IRMS analysis.

### 127 **2.2 Calibration setup and protocol**

128 We developed a two-step calibration procedure to; a) correct for concentration-dependent errors in isotopic data  
129 measurements, and b) correct for deviations in measured  $\delta$ -values from absolute values due to offset (other than  
130 concentration-dependent error) introduced by the laser spectrometer. Also, we used Allan variance curves for  
131 determining the time interval to average the data (Nelson et al., 2008) to achieve the highest precision that can be  
132 offered by LGR-CCIA 36-d (Allan et al., 1997).

133 The first part of our calibration methodology was developed to correct for the concentration-dependent error  
134 observed in preliminary studies for  $\delta^{13}\text{C}$  and  $\delta^{18}\text{O}$  values measured using OA-ICOS. Such a calibration protocol  
135 was used in addition to the routine three-point calibration performed with in-house  $\text{CO}_2$  gas standards of known  
136  $\delta^{13}\text{C}$  and  $\delta^{18}\text{O}$  values. We developed a  $\text{CO}_2$  dilution set up (See Figure. 1), with which each of the three  $\text{CO}_2$   
137 standard gases was diluted with synthetic  $\text{CO}_2$  free air (synth-air) to different  $\text{CO}_2$  concentrations. By applying a  
138 dilution series, we identified the deviation of the measured (OA-ICOS) from the absolute (IRMS)  $\delta^{13}\text{C}$  and  $\delta^{18}\text{O}$   
139 values depending on  $\text{CO}_2$  concentration (See Figure.4). The  $\delta^{13}\text{C}$  and  $\delta^{18}\text{O}$  values of our inhouse calibration gas  
140 standards were measured via cryo-extraction and Dual Inlet IRMS.  $\delta^{13}\text{C}$ , and  $\delta^{18}\text{O}$  of the standard gases (See  
141 Supplementary Table.1) across a wide range of  $\text{CO}_2$  concentrations are measured using OA-ICOS. The deviation  
142 of the measured  $\delta^{13}\text{C}$ , and  $\delta^{18}\text{O}$  from absolute values with respect to changing  $\text{CO}_2$  concentrations was  
143 mathematically modeled and later used for data correction (See Figure.5). A standard three-point calibration was  
144 then applied correcting for concentration-dependent errors (See Figure.7). The standards used covered a wide  
145 range of  $\delta^{13}\text{C}$  and  $\delta^{18}\text{O}$ , including the values observed in the field of application.

146 Standard gases were released to a mass flow controller (ANALYT-MTC, series 358, MFC1) after passing through  
147 a pressure controller valve (See Figure. 1) with safety bypass (TESCOM, D43376-AR-00-X1-S; V5). A Swagelok  
148 filter, ((Stainless Steel All-Welded In-Line Filter (Swagelok, SS-4FWS-05; F1)) was installed at the inlet of the

149 flow controller (ANALYT-MTC, series 358; MFC1). Synth-air was released and passed to another flow controller  
150 (ANALYT-MTC, series 358; MFC2) through a Swagelok filter (F2 in Figure. 1). CO<sub>2</sub> and synth-air leaving the  
151 flow controllers (MFC1 and MFC2 respectively) were then mixed and drawn through a ¼" Teflon tube (P8), which  
152 was kept in a gas thermostat unit (See Figure.1). The thermostat unit contained, a) a thermostat-controlled water  
153 bath (Kottermann, 3082) and b) an Isotherm flask containing liquid nitrogen. The water bath was used to raise the  
154 temperature above room temperature and also to bring the temperature down to +5°C, by placing ice packs in the  
155 water bath. To reach low temperatures (-20°C), we immersed the tubes in the isotherm flask filled with liquid N<sub>2</sub>.  
156 Leaving the thermostat unit, the gas was directed to the multiport inlet unit of the OA-ICOS. By using the  
157 thermostat unit, we introduced a shift in the reference gas temperature and the aim was to test the temperature  
158 sensitivity of the OA-ICOS in measuring δ<sup>13</sup>C and δ<sup>18</sup>O values. The third CO<sub>2</sub> standard gas (which is used for  
159 validation) was produced by mixing the other two gas standards in equal molar proportions in a 10L volume plastic  
160 bag with inner aluminum foil coating and welded seams (CO<sub>2</sub> mix: Linde PLASTIGAS®) under 0.03 MPa pressure  
161 by diluting to the required concentration using synth-air. The mixture was then temperature adjusted and delivered  
162 to the multiport inlet unit (MIU) by using a ¼" Teflon tube (P10). From the multiport inlet unit, calibration gases  
163 were delivered into the OA-ICOS for measurement using a ¼" Teflon tube (P9) at a pressure < 0.0689 MPa, with  
164 a flow rate of 500 mL/min. The gas leaving the OA-ICOS through the exhaust was fed back to the ¼" Teflon tube  
165 (P8) by using a Swagelok pipe Tee (Stainless Steel Pipe Fitting, Male Tee, ¼". Male NPT), intersecting P8 line  
166 before entering the thermostat unit. Thus, the gas fed was looped in the system until steady values were reported  
167 by the OA-ICOS based on CO<sub>2</sub> [ppm], δ<sup>13</sup>C and δ<sup>18</sup>O measurements. CO<sub>2</sub> gas standards were measured at 27  
168 different CO<sub>2</sub> concentration levels ranging between 400 and 25,000 ppm. Every hour before sampling, synth-air  
169 gas was flushed through the system to remove CO<sub>2</sub> to avoid memory effects. The calibration gases were measured  
170 in a sequence one after the other four times. During each round of measurement, every calibration gas was diluted  
171 to different concentrations of CO<sub>2</sub> (400 - 25,000 ppm) and the respective isotopic signature and concentration were  
172 determined. For each measurement of δ<sup>13</sup>C and δ<sup>18</sup>O at a given concentration, the first 50 readings were omitted  
173 to avoid possible memory effects of the laser spectrometer and the subsequent readings for the next 256 seconds  
174 were taken and averaged to get maximum precision for δ<sup>13</sup>C and δ<sup>18</sup>O measurements. When switching between  
175 different calibration gases at the multiport inlet unit, synth-air was purged through the systems for 30 seconds to  
176 avoid cross-contamination.

### 177 **2.3 Experimental Sites**

178 *In situ* experiments were conducted to measure δ<sup>13</sup>C, δ<sup>18</sup>O and concentrations of soil CO<sub>2</sub> in two different soil  
179 types (calcareous and acidic soil). The measurements in a calcareous soil were conducted during June 2014 in  
180 cropland cultivated with wheat (*Triticum aestivum*) in Neuried, a small village in the Upper Rhine Valley in  
181 Germany situated at 48°26'55.5"N, 7°47'20.7"E, 150 m a.s.l. The soil type described as calcareous fluvic Gleysol  
182 developed on gravel deposits in the upper Rhine valley. Soil depth was medium to deep, with high contents of  
183 coarse material (> 2 mm) up to 30 - 50%. Mean soil organic carbon (SOC) content was 1.2 - 2% and, SOC stock

184 was ranging between 50 and 90 t/ha. The average pH was found to be 8.6. The study site receives an annual  
185 rainfall of 810 mm and has a mean annual temperature of 12.1°C.

186 In situ measurements in an acidic soil were conducted by the end of July 2014 in the model ecosystem facility  
187 (MODOEK) of the Swiss Federal Research Institute WSL, Birmensdorf, Switzerland (47°21'48" N, 8°27'23" E,  
188 545 m a.s.l.). The MODOEK facility comprises 16 model ecosystems, belowground split into two lysimeters with  
189 an area of 3 m<sup>2</sup> and a depth of 150 cm. The lysimeters used for the present study were filled with acidic (haplic  
190 Alisol) forest soil and planted with young beech trees (Arend et al., 2016). The soil pH was 4.0 and a total SOC  
191 content of 0.8% (Kuster et al., 2013).

## 192 **2.4 Experimental Setup**

193 The OA-ICOS was connected to gas permeable, hydrophobic membrane tubes (Accurel® tubings, 8 mm OD) of  
194 2 m length, placed horizontally in the soil at different depths. Tubes were laid in six different depths (4, 8, 12, 17,  
195 35, and 80 cm) for calcareous soil and three (10, 30, and 60 cm) for acidic soil.

196 Technical details of the measurement setup are shown in Figure 2. Both ends of the membrane tubes were extended  
197 vertically upwards reaching the soil top by connecting them to gas impermeable Synflex® tubings (8 mm OD)  
198 using Swagelok tube fitting union (Swagelok: SS-8M0-6, 8 mm Tube OD). One end of the tubing system was  
199 connected to a solenoid switching valve (Bibus: MX-758.8E3C3KK) and by using a stainless-steel reducing union  
200 (Swagelok: SS-8M0-6-6M), to the outlet of the LGR CCIA 36-d by using ¼" Teflon tubing. The other end was  
201 connected via the multiport inlet unit to the gas inlet of the LGR CCIA 36-d.

202 This way, a loop was created in which the soil CO<sub>2</sub> drawn into the OA-ICOS was circulated back through the tubes  
203 and in and out of the OA-ICOS and measured until a steady state was reached. We experienced no drop in cavity  
204 pressure while maintaining a closed loop (See Supplementary Figure S2). Each depth was selected and  
205 continuously measured for 6 minutes at specified time intervals by switching to defined depths at the multiport  
206 inlet unit and also at the solenoid valve.

207

## 208 **3 Results and Discussion**

### 209 **3.1 Instrument calibration and correction**

210 The highest level of precision obtained for  $\delta^{13}\text{C}$  and  $\delta^{18}\text{O}$  measurements at the maximum measuring frequency  
211 (1Hz) were determined by using Allan deviation curves (see Figure 3). Maximum precision of 0.022‰ for  $\delta^{13}\text{C}$   
212 was obtained when the data were averaged over 256 seconds, and for  $\delta^{18}\text{O}$ , 0.077‰ for the same averaging interval  
213 as for  $\delta^{13}\text{C}$ .

214 To correct for CO<sub>2</sub> concentration-dependent errors in raw  $\delta^{13}\text{C}$  and  $\delta^{18}\text{O}$  data, we analysed data obtained from the  
215 OA-ICOS to determine the sensitivity of  $\delta^{13}\text{C}$  and  $\delta^{18}\text{O}$  measurements against changing concentrations of CO<sub>2</sub>. We  
216 observed a specific pattern of deviance in the measured isotopic data from the absolute values (both for  $\delta^{13}\text{C}$  and

217  $\delta^{18}\text{O}$ ) across  $\text{CO}_2$  concentration ranging from 25,000 to 400 ppm (See Figure.4). Uncalibrated  $\delta^{13}\text{C}$  and  $\delta^{18}\text{O}$   
218 measurements showed a standard deviation of 6.44 ‰ and 6.802 ‰ respectively, when measured under changing  
219  $\text{CO}_2$  concentrations.

220 The dependency of  $\delta^{13}\text{C}$  and  $\delta^{18}\text{O}$  values on the  $\text{CO}_2$  concentration was compensated by using a nonlinear model.  
221 The deviations (Diff- $\delta$ ) of the measured delta values ( $\delta_{(\text{OA-ICOS})}$ ) from the absolute value of the standard gas ( $\delta_{(\text{IRMS})}$ )  
222 at different concentrations of  $\text{CO}_2$  were calculated (Diff- $\delta = \delta_{(\text{OA-ICOS})} - \delta_{(\text{IRMS})}$ ). Several mathematical  
223 models were then fitted on Diff- $\delta$  as a function of changing  $\text{CO}_2$  concentration (See figure.5). The mathematical  
224 model with the best fit for Diff- $\delta$  data was selected using Akaike information criterion corrected (AICc) (Glatting  
225 et al., 2007; Hurvich and Tsai, 1989; Yamaoka et al., 1978). The non-linear model fits applied for Diff- $\delta^{13}\text{C}$ , and  
226 Diff- $\delta^{18}\text{O}$  measurements are given in Tables 1 & 2, respectively. For Diff- $\delta^{13}\text{C}$ , a three-parameter exponential  
227 model fitted best with  $r^2 = 0.99$  (see Table 3 for the values of the parameters, see supplementary Figure S3 (a) for  
228 model residuals), and a three-parameter power function model (see Table 2) with  $r^2 = 0.99$  showed the best fit for  
229 Diff- $\delta^{18}\text{O}$  (see Table 3 for the values of the parameters, see supplementary Figure S3 (b) for model residuals). The  
230 best fit was then introduced into the measured isotopic data ( $\delta^{13}\text{C}$  and  $\delta^{18}\text{O}$ ) and corrected for concentration-  
231 dependent errors (See figure. 6). After correction, the standard deviation of  $\delta^{13}\text{C}$  was reduced to 0.08 ‰ and of  
232  $\delta^{18}\text{O}$  to 0.09 ‰ for all measurements across the whole  $\text{CO}_2$  concentration range.

233  
234 After correcting the measured  $\delta^{13}\text{C}$  and  $\delta^{18}\text{O}$  values for the  $\text{CO}_2$  concentration-dependent deviations, a three-point  
235 calibration (Sturm et al., 2012) was made by generating linear regressions with the concentration corrected  $\delta^{13}\text{C}$   
236 and  $\delta^{18}\text{O}$  values against absolute  $\delta^{13}\text{C}$  and  $\delta^{18}\text{O}$  values (See Figure.7, see supplementary Figure S4 for linear  
237 regression residuals). Using the linear regression lines, we were able to measure the validation gas standard with  
238 standard deviations of 0.0826 ‰ for  $\delta^{13}\text{C}$  and 0.0941 ‰ for  $\delta^{18}\text{O}$ .

239 For the LGR CCIA 36-d, we found that routine calibration (Correction for concentration-dependent error plus  
240 three-point calibration) was **necessary** for obtaining the required accuracy, in particular under fluctuating  $\text{CO}_2$   
241 concentrations. The LGR CCIA-36d offers an option for calibration against a single standard, a feature which was  
242 already in place in a predecessor model (CCIA DLT-100) (Guillon et al., 2012). This internal calibration is  
243 sufficient, when LGR CCIA-36d is operated only under stable  $\text{CO}_2$  concentrations. To correct for the concentration  
244 dependency, we introduced mathematical model fits, which corrected for the deviation pattern found for both  $\delta^{13}\text{C}$   
245 and  $\delta^{18}\text{O}$ . We assume that these deviations are instrument specific and the fitting parameters need to be adjusted  
246 for every single device. Experiments conducted to investigate the influence of external temperature fluctuations  
247 on OA-ICOS measurements did not show any significant changes in the temperature inside the optical cavity of  
248 OA-ICOS (See Supplementary Figure S1). The previous version of the Los Gatos CCIA was strongly influenced  
249 by temperature fluctuations during sampling (Guillon et al., 2012). The lack of temperature dependency as  
250 observed here with the most recent model can be mostly due to the heavy insulation provided with the system,  
251 which was not found in the older models.

252 Guillon et al. (2012) found a linear correlation between  $\text{CO}_2$  concentration and respective stable isotope signatures  
253 with a previous version of the Los Gatos CCIA  $\text{CO}_2$  stable isotope analyser. In our experiments with the OA-ICOS,  
254 best fitting correlation between  $\text{CO}_2$  concentration and  $\delta^{13}\text{C}$  and  $\delta^{18}\text{O}$  measurements were exponential and power

255 functions, respectively. We assume that measurement accuracy is influenced by the number of CO<sub>2</sub> molecules  
256 present inside the laser cavity of the particular laser spectrometer as we observed large standard deviation in  
257 isotopic measurements at lower CO<sub>2</sub> concentrations. This behavior of an OA-ICOS can be expected as it functions  
258 by sweeping the laser along an absorption spectrum, measuring the energy transmitted after passing through the  
259 sample. Therefore, energy transmitted is proportional to the gas concentration in the cavity. The laser absorbance  
260 is then determined by normalizing against a reference signal, finally calculating the concentration of the sample  
261 measured by integrating the whole spectrum of absorbance (O'Keefe et al., 1999).

### 262 3.2 Variation in soil CO<sub>2</sub> concentration, carbon and oxygen isotope values

263 Figures 9 and 10 show the CO<sub>2</sub> concentration,  $\delta^{13}\text{C}$  and  $\delta^{18}\text{O}$  measurements of soil CO<sub>2</sub> in the calcareous as well  
264 as in the acidic soil across the soil profile with sub-daily resolution and as averages for the day, respectively. We  
265 observed an increase in the CO<sub>2</sub> concentration across the soil depth profile for both, the calcareous and the acidic  
266 soil. Moreover, there were rather contrasting  $\delta^{13}\text{C}$  values across the profile for the two soil types. In the calcareous  
267 soil, CO<sub>2</sub> was relatively enriched in <sup>13</sup>C in the surface soil (4 cm) as compared to the 8 cm depth. Below 8 cm down  
268 to 80 cm depth, we found an increase in  $\delta^{13}\text{C}$  values. At 80 cm depth, the  $\delta^{13}\text{C}$  in soil CO<sub>2</sub> ranged between -7.15  
269 and -3.35 ‰ (See Figure. 9) with a daily average of  $-6.19 \pm 1.45$  ‰ (See Figure. 10) and hence clearly above  
270 atmospheric values ( $\approx -8.0$  ‰). For  $\delta^{18}\text{O}$  values of calcareous soil, the depth profile showed no specific pattern  
271 except for the  $\delta^{18}\text{O}$  values at 80 cm depth was found to be less negative than the values of the other depths. The  
272  $\delta^{18}\text{O}$  value in the top 4 cm was found to be slightly more enriched than the 8 cm depth and between 8 cm – 35 cm,  
273  $\delta^{18}\text{O}$  values showed little variation relative to each other. For the sub-daily measurements, we observed a sharp  
274 decline in  $\delta^{18}\text{O}$  values at around 02:00, which is also observed but less pronounced for  $\delta^{13}\text{C}$  signal. We assume  
275 that, the reason for such aberrant values is rather a technical issue than a biological process. It could be due to the  
276 fact that the internal pump in the OA-ICOS was not taking adequate amount of gas into the optical cavity, thereby  
277 creating a negative pressure inside the cavity resulting in the observed aberrant values. The patterns observed for  
278 the  $\delta^{13}\text{C}$  values of CO<sub>2</sub> in the calcareous soil with <sup>13</sup>C enrichment in deeper soil layers can be explained by a  
279 substantial contribution of CO<sub>2</sub> from abiotic origin to total soil CO<sub>2</sub> release as a result of carbonate weathering and  
280 subsequent out-gassing from soil water (Schindlbacher et al., 2015). According to Cerling (1984), the distinct  
281 oxygen and carbon isotopic composition of soil carbonate depends primarily on the isotopic signature of meteoric  
282 water and to the proportion of C<sub>4</sub> biomass present at the time of carbonate formation (Cerling, 1984), but also on  
283 numerous other factors that determine the <sup>13</sup>C value of soil CO<sub>2</sub>. CO<sub>2</sub> released as a result from carbonates in  
284 calcareous soil site have a distinct  $\delta^{13}\text{C}$  value of -9.313 (mean value across soil profile 0 - 80 cm depth) (Figure  
285 8(c)), while CO<sub>2</sub> released during biological respiratory processes has  $\delta^{13}\text{C}$  values around -24‰ as observed in the  
286 acidic soil (Figure 10 (e)). The carbonate  $\delta^{13}\text{C}$  values observed in the calcareous soil site was indicative of presence  
287 of carbonate sources of pedogenic and geologic origin. Even though the contribution of CO<sub>2</sub> from abiotic sources  
288 to soil CO<sub>2</sub> is often considered to be low, several studies have reported significant proportions ranging between  
289 (10 - 60%) emanating from abiotic sources (Emmerich, 2003; Plestenjak et al., 2012; Ramnarine et al., 2012;  
290 Serrano-Ortiz et al., 2010; Stevenson and Verburg, 2006; Tamir et al., 2011). Bowen and Beerling, (2004) showed  
291 that isotope effects associated with soil organic matter decomposition can cause a strong gradient in  $\delta$  values of  
292 soil organic matter (SOM) with depth, but are not always reflected in the  $\delta^{13}\text{C}$  values of soil CO<sub>2</sub>. We have

293 measured soil samples for bulk soil  $\delta^{13}\text{C}$ , carbonate  $\delta^{13}\text{C}$  &  $\delta^{18}\text{O}$  values and also determined the percentage of total  
294 carbon in the soil across a depth profile of (0-80 cm) (See Figure 8). We observed an increase in  $\delta^{13}\text{C}$  values for  
295 bulk soil in deeper soil layers (See Figure 8 (a,c)). Moreover, also the carbonate  $\delta^{13}\text{C}$  values got more positive in  
296 the 60-80 cm layer. Since total organic carbon content decreases with depth it can be assumed that  $\text{CO}_2$  derived  
297 from carbonate weathering having less negative  $\delta^{13}\text{C}$  more strongly contributed to the soil  $\text{CO}_2$  (especially since  
298 we see an increase in soil  $\text{CO}_2$  concentration with depth). This is accordance with the laser-based measurements  
299 which showed a strong increase in  $\delta^{13}\text{C}$  of soil  $\text{CO}_2$  in the deepest soil layer leading us to the hypothesis that this  
300 signal is indicating a strong contribution of carbonate derived  $\text{CO}_2$ . Water content, soil  $\text{CO}_2$  concentration and  
301 presence of organic acids or any other source of  $\text{H}^+$  are the major factors influencing carbonate weathering, and  
302 variations in soil  $\text{CO}_2$  partial pressure, moisture, temperature, and pH can cause degassing of  $\text{CO}_2$  which  
303 contributes to the soil  $\text{CO}_2$  efflux (Schindlbacher et al., 2015; Zamanian et al., 2016).  $\text{CaCO}_3$  solubility in pure  
304  $\text{H}_2\text{O}$  at  $25^\circ\text{C}$  is  $0.013 \text{ gL}^{-1}$ , but in weak acids like carbonic acid, the solubility is increased up to five fold (Zamanian  
305 et al., 2016). The production of carbonic acid due to  $\text{CO}_2$  dissolution will convert carbonate to bicarbonates  
306 resulting in exchange of carbon atoms between carbonates and dissolved  $\text{CO}_2$ . We assume that at our study site,  
307 the topsoil is de-carbonated due to intensive agriculture for a longer period and thus soil  $\text{CO}_2$  there originates  
308 primarily from autotrophic and heterotrophic respiratory activity. In contrast to the deeper soil layers, where the  
309 carbonate content is high,  $\text{CO}_2$  from carbonate weathering is assumed to be a dominating source of soil  $\text{CO}_2$ . Also,  
310 outgassing of  $\text{CO}_2$  from the large groundwater body underneath the calcareous Gleysol might contribute to the  
311 inorganic  $\text{CO}_2$  sources in the deeper soil as we found ground water table to be 1-2m below the soil surface. Relative  
312  $^{13}\text{C}$  enrichment of the  $\text{CO}_2$  in the topsoil (4 cm) compared to 8 cm depth is probably due to the invasive diffusion  
313 of atmospheric  $\text{CO}_2$  which has a  $\delta^{13}\text{C}$  value close to  $-8\text{‰}$  (e.g., (Levin et al., 1995) ). The  $\delta^{18}\text{O}$  patterns for  $\text{CO}_2$   
314 between 4 and 35 cm might reflect the  $\delta^{18}\text{O}$  of soil water with stronger evaporative enrichment at the top and  $^{18}\text{O}$   
315 depletion towards deeper soil layers. In comparison, the strong  $^{18}\text{O}$  enrichment of soil  $\text{CO}_2$  towards 80 cm in the  
316 calcareous Gleysol very likely reflects the  $^{18}\text{O}$  values of groundwater lending further support for the high  
317 contribution of  $\text{CO}_2$  originating from the outgassing of groundwater. We, however, need then to assume that that  
318 the oxygen in the  $\text{CO}_2$  is not in full equilibrium with the precipitation influenced soil water. As mainly microbial  
319 carbonic anhydrase mediates the fast equilibrium between  $\text{CO}_2$  and water in the soil and the microbial activity is  
320 low in deeper soil layers (Schmidt et al., 2011), we speculate that in deep layers with a significant contribution of  
321 ground-water derived  $\text{CO}_2$  to the  $\text{CO}_2$  pool, a lack of full equilibration with soil water might be the reason for the  
322 observed  $\delta^{18}\text{O}$  values.

323  
324 Soil  $\text{CO}_2$  concentration in the acidic soil showed a positive relationship with soil depth as  $\text{CO}_2$  concentration  
325 increased along with increasing soil depth (Figs. 9 & 10).  $\text{CO}_2$  concentrations were distinctly higher than in the  
326 calcareous soil, very likely due to the finer texture than in the gravel-rich calcareous soil.  $\delta^{13}\text{C}$  values amounted to  
327 approx.  $-26 \text{‰}$  in 30 and 60 cm depth indicating the biotic origin from (autotrophic and heterotrophic) soil  
328 respiration (Schönwitz et al., 1986). In the topsoil,  $\delta^{13}\text{C}$  values did not strongly increase, pointing towards a less  
329 pronounced inward diffusion of  $\text{CO}_2$  in the acidic soil site, most likely due to more extensive outward diffusion of  
330 soil  $\text{CO}_2$  as indicated by the still very high  $\text{CO}_2$  concentration at 10 cm creating a sharp gradient between soil and  
331 atmosphere. Moreover, the acidic soil was rather dense and contained no stones, strongly suggesting that gas

332 diffusivity was rather small.  $\delta^{18}\text{O}$  depths patterns of soil  $\text{CO}_2$  in the acidic soil were most likely reflecting  $\delta^{18}\text{O}$   
333 values of soil water as  $\text{CO}_2$  became increasingly  $^{18}\text{O}$  depleted from top to bottom.  $\delta^{18}\text{O}$  of deeper soil layers  $\text{CO}_2$   
334 (30 - 60 cm) was close to the values expected when full oxygen exchange between soil water and  $\text{CO}_2$  occurred  
335 (Kato et al., 2004). Assuming an  $^{18}\text{O}$  fractionation of 41‰ between  $\text{CO}_2$  and water (Brenninkmeijer et al., 1983)  
336 this would result in an expected value for  $\text{CO}_2$  of  $\approx -10 \pm 2\%$  vs. VPDB- $\text{CO}_2$ . Corresponding results had been  
337 shown for  $\delta^{18}\text{O}$  of soil  $\text{CO}_2$  using similar hydrophobic gas permeable membrane tubes used when measuring  $\delta^{18}\text{O}$   
338 of soil  $\text{CO}_2$  and soil water *in situ* (Gangi et al., 2015).

#### 339 4 Conclusions

340 During our preliminary tests with the OA-ICOS, we found that the equipment was highly sensitive to changes in  
341  $\text{CO}_2$  concentrations. We found a non-linear response of the  $\delta^{13}\text{C}$  and  $\delta^{18}\text{O}$  values against changes in  $\text{CO}_2$   
342 concentration. Given the fact that laser-based  $\text{CO}_2$  isotope analyzers are deployed on site in combination with  
343 different gas sampling methods like automated chambers systems (Bowling et al., 2015), and hydrophobic gas  
344 permeable membranes (Jochheim et al., 2018) for tracing various ecosystem processes, it is important to address  
345 this issue. Therefore, we developed a calibration strategy for correcting errors introduced in  $\delta^{13}\text{C}$  and  $\delta^{18}\text{O}$   
346 measurements due to the sensitivity of the device against changing  $\text{CO}_2$  concentrations. We found that the OA-  
347 ICOS measures stable isotopes of  $\text{CO}_2$  gas samples with a precision comparable to conventional IRMS. The  
348 method described in this work for measuring  $\text{CO}_2$  concentration,  $\delta^{13}\text{C}$  and  $\delta^{18}\text{O}$  values in soil air profiles using an  
349 OA-ICOS and hydrophobic gas permeable tubes are promising and can be applied for soil  $\text{CO}_2$  flux studies. As  
350 this set up is capable of measuring continuously for longer time periods at higher temporal resolution (0.05 – 0.1  
351 Hz), it offers greater potential to investigate the isotopic identity of  $\text{CO}_2$  and the interrelation between soil  $\text{CO}_2$  and  
352 soil water. By using our measurement setup, we could identify abiotic as well as biotic contributions to the soil  
353  $\text{CO}_2$  in the calcareous soil. We infer that that degassing of  $\text{CO}_2$  from carbonates due to weathering and evasion of  
354  $\text{CO}_2$  from groundwater may leave the soil  $\text{CO}_2$  with a specific and distinct  $\delta^{13}\text{C}$  signature especially when the biotic  
355 activity is rather low.

356

357

#### 358 Acknowledgements

359 We thank Federal Ministry of Education and Research, Germany (BMBF), KIT (Karlsruhe Institute of  
360 Technology) for providing financial support for the project ENABLE-WCM (Grant Number: 02WQ1205). AG  
361 and JJ acknowledge financial support by the Swiss National Science Foundation (SNF; 31003A\_159866). We  
362 thank Barbara Herbstritt, Hannes Leistert, Emil Blattmann and Jens Lange, Matthias Saurer, Alessandro Schlumpf,  
363 Lukas Bächli and Christian Poll for outstanding support in getting this project into a reality.

364

365

366

367  
368  
369  
370  
371  
372  
373  
374  
375  
376  
377  
378  
379  
380  
381  
382  
383  
384  
385  
386  
387  
388  
389  
390  
391  
392  
393  
394  
395  
396

**References**

Allan, D. W., Ashby, N. and Hodge, C. C.: The Science of Timekeeping, Hewlett-Packard, 88  
[online] Available from:  
[http://www.allanstime.com/Publications/DWA/Science\\_Timekeeping/TheScienceOfTimekeeping.pdf](http://www.allanstime.com/Publications/DWA/Science_Timekeeping/TheScienceOfTimekeeping.pdf), 1997.

Arend, M., Gessler, A. and Schaub, M.: The influence of the soil on spring and autumn phenology in European beech, edited by C. Li, *Tree Physiol.*, 36(1), 78–85, doi:10.1093/treephys/tpv087, 2016.

Baer, D. S., Paul, J. B., Gupta, M. and O’Keefe, A.: Sensitive absorption measurements in the near-infrared region using off-axis integrated-cavity-output spectroscopy, *Appl. Phys. B Lasers Opt.*, 75(2–3), 261–265, doi:10.1007/s00340-002-0971-z, 2002.

Barthel, M., Sturm, P., Hammerle, A., Buchmann, N., Gentsch, L., Siegwolf, R. and Knohl, A.: Soil H<sub>2</sub> 18 O labelling reveals the effect of drought on C 18 OO fluxes to the atmosphere, *J. Exp. Bot.*, 65(20), 5783–5793, doi:10.1093/jxb/eru312, 2014.

von Basum, G., Halmer, D., Hering, P., Mürtz, M., Schiller, S., Müller, F., Popp, A. and Kühnemann, F.: Parts per trillion sensitivity for ethane in air with an optical parametric oscillator cavity leak-out spectrometer, *Opt. Lett.*, 29(8), 797, doi:10.1364/OL.29.000797, 2004.

Bertolini, T., Inghima, I., Rubino, M., Marzaioli, F., Lubritto, C., Subke, J.-A., Peressotti, A. and Cotrufo, M. F.: Sampling soil-derived CO<sub>2</sub> for analysis of isotopic composition: a comparison of different techniques, *Isotopes Environ. Health Stud.*, 42(1), 57–65, doi:10.1080/10256010500503312, 2006.

397 Bond-Lamberty, B. and Thomson, A.: Temperature-associated increases in the global soil  
398 respiration record, *Nature*, 464(7288), 579–582, doi:10.1038/nature08930, 2010.

399 Bowen, G. J. and Beerling, D. J.: An integrated model for soil organic carbon and CO<sub>2</sub>:  
400 Implications for paleosol carbonate *p* CO<sub>2</sub> paleobarometry, *Global Biogeochem. Cycles*, 18(1),  
401 n/a-n/a, doi:10.1029/2003GB002117, 2004.

402 Bowling, D. R., Sargent, S. D., Tanner, B. D. and Ehleringer, J. R.: Tunable diode laser  
403 absorption spectroscopy for stable isotope studies of ecosystem–atmosphere CO<sub>2</sub> exchange,  
404 *Agric. For. Meteorol.*, 118(1–2), 1–19, doi:10.1016/S0168-1923(03)00074-1, 2003.

405 Bowling, D. R., Egan, J. E., Hall, S. J. and Risk, D. A.: Environmental forcing does not induce  
406 diel or synoptic variation in the carbon isotope content of forest soil respiration, *Biogeosciences*,  
407 12, 5143–5160, doi:10.5194/bg-12-5143-2015, 2015.

408 Breecker, D. and Sharp, Z. D.: A field and laboratory method for monitoring the concentration  
409 and isotopic composition of soil CO<sub>2</sub>, *Rapid Commun. Mass Spectrom.*, 22(4), 449–454,  
410 doi:10.1002/rcm.3382, 2008.

411 Brenninkmeijer, C. A. M., Kraft, P. and Mook, W. G.: Oxygen isotope fractionation between  
412 CO<sub>2</sub> and H<sub>2</sub>O, *Chem. Geol.*, 41, 181–190, doi:10.1016/S0009-2541(83)80015-1, 1983.

413 Cerling, T. E.: The stable isotopic composition of modern soil carbonate and its relationship to  
414 climate, *Earth Planet. Sci. Lett.*, 71(2), 229–240, doi:10.1016/0012-821X(84)90089-X, 1984.

415 Emmerich, W. E.: Carbon dioxide fluxes in a semiarid environment with high carbonate soils,  
416 *Agric. For. Meteorol.*, 116, 91–102 [online] Available from:  
417 <http://citeseerx.ist.psu.edu/viewdoc/download?doi=10.1.1.457.6452&rep=rep1&type=pdf>,  
418 2003.

419 Francey, R. J. and Tans, P. P.: Latitudinal variation in oxygen-18 of atmospheric CO<sub>2</sub>, *Nature*,  
420 327(6122), 495–497, doi:10.1038/327495a0, 1987.

421 Gangi, L., Rothfuss, Y., Ogée, J., Wingate, L., Vereecken, H. and Brüggemann, N.: A New  
422 Method for In Situ Measurements of Oxygen Isotopologues of Soil Water and Carbon Dioxide  
423 with High Time Resolution, *Vadose Zo. J.*, 14(8), 0, doi:10.2136/vzj2014.11.0169, 2015.

424 Glatting, G., Kletting, P., Reske, S. N., Hohl, K. and Ring, C.: Choosing the optimal fit function:  
425 Comparison of the Akaike information criterion and the F-test, *Med. Phys.*, 34(11), 4285–4292,  
426 doi:10.1118/1.2794176, 2007.

427 Guillon, S., Pili, E. and Agrinier, P.: Using a laser-based CO<sub>2</sub> carbon isotope analyser to  
428 investigate gas transfer in geological media, *Appl. Phys. B*, 107(2), 449–457,  
429 doi:10.1007/s00340-012-4942-8, 2012.

430 Gut, A., Blatter, A., Fahrni, M., Lehmann, B. E., Neftel, A. and Staffelbach, T.: A new  
431 membrane tube technique (METT) for continuous gas measurements in soils, *Plant Soil*, 198(1),  
432 79–88, doi:10.1023/A:1004277519234, 1998.

433 Harwood, K. G., Gillon, J. S., Roberts, A. and Griffiths, H.: Determinants of isotopic coupling  
434 of CO<sub>2</sub> and water vapour within a *Quercus petraea* forest canopy, *Oecologia*, 119(1), 109–119,  
435 doi:10.1007/s004420050766, 1999.

436 Hurvich, C. M. and Tsai, C.: Regression and time series model selection in small samples,  
437 *Biometrika*, 76(2), 297–307, doi:10.1093/biomet/76.2.297, 1989.

438 Jochheim, H., Wirth, S. and von Unold, G.: A multi-layer, closed-loop system for continuous  
439 measurement of soil CO<sub>2</sub> concentration, *J. Plant Nutr. Soil Sci.*, 181(1), 61–68,  
440 doi:10.1002/jpln.201700259, 2018.

441 Jost, H.-J., Castrillo, A. and Wilson, H. W.: Simultaneous <sup>13</sup>C/ <sup>12</sup>C and <sup>18</sup>O/ <sup>16</sup>O isotope ratio  
442 measurements on CO<sub>2</sub> based on off-axis integrated cavity output spectroscopy, *Isotopes*  
443 *Environ. Health Stud.*, 42(1), 37–45, doi:10.1080/10256010500503163, 2006.

444 Kammer, A., Tuzson, B., Emmenegger, L., Knohl, A., Mohn, J. and Hagedorn, F.: Application  
445 of a quantum cascade laser-based spectrometer in a closed chamber system for real-time δ<sup>13</sup>C  
446 and δ<sup>18</sup>O measurements of soil-respired CO<sub>2</sub>, *Agric. For. Meteorol.*, 151(1), 39–48,  
447 doi:10.1016/j.agrformet.2010.09.001, 2011.

448 Kato, T., Nakazawa, T., Aoki, S., Sugawara, S. and Ishizawa, M.: Seasonal variation of the  
449 oxygen isotopic ratio of atmospheric carbon dioxide in a temperate forest, Japan, ,  
450 doi:10.1029/2003GB002173, 2004.

451 Kayler, Z. E., Sulzman, E. W., Rugh, W. D., Mix, A. C. and Bond, B. J.: Soil biology and  
452 biochemistry., Pergamon. [online] Available from:  
453 <https://www.cabdirect.org/cabdirect/abstract/20103097455> (Accessed 16 March 2018), 2010.

454 Keeling, C. D.: The concentration and isotopic abundances of atmospheric carbon dioxide in  
455 rural areas, *Geochim. Cosmochim. Acta*, 13(4), 322–334, doi:10.1016/0016-7037(58)90033-4,  
456 1958.

457 Kerstel, E. and Gianfrani, L.: Advances in laser-based isotope ratio measurements: selected  
458 applications, *Appl. Phys. B*, 92(3), 439–449, doi:10.1007/s00340-008-3128-x, 2008.

459 Kuster, T. M., Arend, M., Bleuler, P., Günthardt-Goerg, M. S. and Schulin, R.: Water regime  
460 and growth of young oak stands subjected to air-warming and drought on two different forest  
461 soils in a model ecosystem experiment, *Plant Biol.*, 15, 138–147, doi:10.1111/j.1438-  
462 8677.2011.00552.x, 2013.

463 Kuzyakov, Y.: Sources of CO<sub>2</sub> efflux from soil and review of partitioning methods, *Soil Biol.*  
464 *Biochem.*, 38(3), 425–448, doi:10.1016/j.soilbio.2005.08.020, 2006.

465 Levin, I., Graul, R. and Trivett, N. B. A.: Long-term observations of atmospheric CO<sub>2</sub> and  
466 carbon isotopes at continental sites in Germany, *Tellus B*, 47(1–2), 23–34, doi:10.1034/j.1600-  
467 0889.47.issue1.4.x, 1995.

468 Maier, M. and Schack-Kirchner, H.: Using the gradient method to determine soil gas flux: A  
469 review, *Agric. For. Meteorol.*, 192–193, 78–95, doi:10.1016/j.agrformet.2014.03.006, 2014.

470 Mortazavi, B., Prater, J. L. and Chanton, J. P.: A field-based method for simultaneous  
471 measurements of the  $\delta^{18}\text{O}$  and  $\delta^{13}\text{C}$  of soil CO<sub>2</sub> efflux, *Biogeosciences*, 1(1), 1–9,  
472 doi:10.5194/bg-1-1-2004, 2004.

473 Nelson, D. D., McManus, J. B., Herndon, S. C., Zahniser, M. S., Tuzson, B. and Emmenegger,  
474 L.: New method for isotopic ratio measurements of atmospheric carbon dioxide using a 4.3  $\mu\text{m}$   
475 pulsed quantum cascade laser, *Appl. Phys. B*, 90(2), 301–309, doi:10.1007/s00340-007-2894-  
476 1, 2008.

477 O’Keefe, A. and Deacon, D. A. G.: Cavity ring-down optical spectrometer for absorption  
478 measurements using pulsed laser sources, *Rev. Sci. Instrum.*, 59(12), 2544–2551,  
479 doi:10.1063/1.1139895, 1988.

480 Oerter, E. J. and Amundson, R.: Climate controls on spatial and temporal variations in the  
481 formation of pedogenic carbonate in the western Great Basin of North America, *Geol. Soc. Am.*  
482 *Bull.*, 128(7–8), 1095–1104, doi:10.1130/B31367.1, 2016.

483 Ohlsson, K., Singh, B., Holm, S., Nordgren, A., Lovdahl, L. and Hogberg, P.: Uncertainties in  
484 static closed chamber measurements of the carbon isotopic ratio of soil-respired CO, *Soil Biol.*  
485 *Biochem.*, 37(12), 2273–2276, doi:10.1016/j.soilbio.2005.03.023, 2005.

486 Parameswaran, K. R., Rosen, D. I., Allen, M. G., Ganz, A. M. and Risby, T. H.: Off-axis

487 integrated cavity output spectroscopy with a mid-infrared interband cascade laser for real-time  
488 breath ethane measurements, *Appl. Opt.*, 48(4), B73, doi:10.1364/AO.48.000B73, 2009.

489 Parent, F., Plain, C., Epron, D., Maier, M. and Longdoz, B.: A new method for continuously  
490 measuring the  $\delta^{13}\text{C}$  of soil  $\text{CO}_2$  concentrations at different depths by laser spectrometry, *Eur.*  
491 *J. Soil Sci.*, 64(4), 516–525, doi:10.1111/ejss.12047, 2013.

492 Peltola, J., Vainio, M., Ulvila, V., Siltanen, M., Metsälä, M. and Halonen, L.: Off-axis re-entrant  
493 cavity ring-down spectroscopy with a mid-infrared continuous-wave optical parametric  
494 oscillator, *Appl. Phys. B*, 107(3), 839–847, doi:10.1007/s00340-012-5074-x, 2012.

495 Plestenjak, G., Eler, K., Vodnik, D., Ferlan, M., Čater, M., Kanduč, T., Simončič, P. and Ogrinc,  
496 N.: Sources of soil  $\text{CO}_2$  in calcareous grassland with woody plant encroachment, *J. Soils*  
497 *Sediments*, 12(9), 1327–1338, doi:10.1007/s11368-012-0564-3, 2012.

498 Ramnarine, R., Wagner-Riddle, C., Dunfield, K. E. and Voroney, R. P.: Contributions of  
499 carbonates to soil  $\text{CO}_2$  emissions, *Can. J. Soil Sci.*, 92(4), 599–607, doi:10.4141/cjss2011-025,  
500 2012.

501 Risk, D. and Kellman, L.: Isotopic fractionation in non-equilibrium diffusive environments,  
502 *Geophys. Res. Lett.*, 35(2), L02403, doi:10.1029/2007GL032374, 2008.

503 Satakhun, D., Gay, F., Chairungsee, N., Kasemsap, P., Chantuma, P., Thanisawanyangkura, S.,  
504 Thaler, P. and Epron, D.: Soil  $\text{CO}_2$  efflux and soil carbon balance of a tropical rubber plantation,  
505 *Ecol. Res.*, 28(6), 969–979, doi:10.1007/s11284-013-1079-0, 2013.

506 Schär, C., Vidale, P. L., Lüthi, D., Frei, C., Häberli, C., Liniger, M. A. and Appenzeller, C.:  
507 The role of increasing temperature variability in European summer heatwaves, *Nature*,  
508 427(6972), 332–336, doi:10.1038/nature02300, 2004.

509 Schindlbacher, A., Borken, W., Djukic, I., Brandstätter, C., Spötl, C. and Wanek, W.:  
510 Contribution of carbonate weathering to the  $\text{CO}_2$  efflux from temperate forest soils,  
511 *Biogeochemistry*, 124(1–3), 273–290, doi:10.1007/s10533-015-0097-0, 2015.

512 Schmidt, M. W. I., Torn, M. S., Abiven, S., Dittmar, T., Guggenberger, G., Janssens, I. A.,  
513 Kleber, M., Kögel-Knabner, I., Lehmann, J., Manning, D. A. C., Nannipieri, P., Rasse, D. P.,  
514 Weiner, S. and Trumbore, S. E.: Persistence of soil organic matter as an ecosystem property,  
515 *Nature*, 478(7367), 49–56, doi:10.1038/nature10386, 2011.

516 Schönwitz, R., Stichler, W. and Ziegler, H.:  $\delta^{13}\text{C}$  values of  $\text{CO}_2$  from soil respiration on sites

517 with crops of C3 and C4 type of photosynthesis, *Oecologia*, 69(2), 305–308,  
518 doi:10.1007/BF00377638, 1986.

519 Serrano-Ortiz, P., Roland, M., Sanchez-Moral, S., Janssens, I. A., Domingo, F., Godd ris, Y.  
520 and Kowalski, A. S.: Hidden, abiotic CO2 flows and gaseous reservoirs in the terrestrial carbon  
521 cycle: Review and perspectives, *Agric. For. Meteorol.*, 150(3), 321–329,  
522 doi:10.1016/j.agrformet.2010.01.002, 2010.

523 Sperber, C. Von, Weiler, M. and B ggemann, N.: The effect of soil moisture, soil particle size,  
524 litter layer and carbonic anhydrase on the oxygen isotopic composition of soil-released CO2,  
525 *Eur. J. Soil Sci.*, doi:10.1111/ejss.12241, 2015.

526 Stevenson, B. A. and Verburg, P. S. J.: Effluxed CO2-13C from sterilized and unsterilized  
527 treatments of a calcareous soil, *Soil Biol. Biochem.*, 38(7), 1727–1733,  
528 doi:10.1016/j.soilbio.2005.11.028, 2006.

529 Stumpp, C., Br ggemann, N. and Wingate, L.: Stable Isotope Approaches in Vadose Zone  
530 Research, *Vadose Zo. J.*, 17(1), 0, doi:10.2136/vzj2018.05.0096, 2018.

531 Sturm, P., Eugster, W. and Knohl, A.: Eddy covariance measurements of CO2 isotopologues  
532 with a quantum cascade laser absorption spectrometer, *Agric. For. Meteorol.*, 152, 73–82,  
533 doi:10.1016/j.agrformet.2011.09.007, 2012.

534 Tamir, G., Shenker, M., Heller, H., Bloom, P. R., Fine, P. and Bar-Tal, A.: Can Soil Carbonate  
535 Dissolution Lead to Overestimation of Soil Respiration?, *Soil Sci. Soc. Am. J.*, 75(4), 1414,  
536 doi:10.2136/sssaj2010.0396, 2011.

537 Torn, M. S., Davis, S., Bird, J. A., Shaw, M. R. and Conrad, M. E.: Automated analysis  
538 of 13C/12C ratios in CO2 and dissolved inorganic carbon for ecological and environmental  
539 applications, *Rapid Commun. Mass Spectrom.*, 17(23), 2675–2682, doi:10.1002/rcm.1246,  
540 2003.

541 Werner, C. and Gessler, A.: Diel variations in the carbon isotope composition of respired CO2  
542 and associated carbon sources: a review of dynamics and mechanisms, *Biogeosciences*, 8(9),  
543 2437–2459, doi:10.5194/bg-8-2437-2011, 2011.

544 Werner, C., Schnyder, H., Cuntz, M., Keitel, C., Zeeman, M. J., Dawson, T. E., Badeck, F. W.,  
545 Brugnoli, E., Ghashghaie, J., Grams, T. E. E., Kayler, Z. E., Lakatos, M., Lee, X., M guas, C.,  
546 Og e, J., Rascher, K. G., Siegwolf, R. T. W., Unger, S., Welker, J., Wingate, L. and Gessler,

547 A.: Progress and challenges in using stable isotopes to trace plant carbon and water relations  
548 across scales, *Biogeosciences*, 9(8), 3083–3111, doi:10.5194/bg-9-3083-2012, 2012.

549 Wingate, L., Ogée, J., Cuntz, M., Genty, B., Reiter, I., Seibt, U., Yakir, D., Maseyk, K., Pendall,  
550 E. G., Barbour, M. M., Mortazavi, B., Burlett, R., Peylin, P., Miller, J., Mencuccini, M., Shim,  
551 J. H., Hunt, J. and Grace, J.: The impact of soil microorganisms on the global budget of  
552 delta18O in atmospheric CO<sub>2</sub>, *Proc. Natl. Acad. Sci. U. S. A.*, 106(52), 22411–5,  
553 doi:10.1073/pnas.0905210106, 2009.

554 Wingate, L., Ogée, J., Burlett, R., Bosc, A., Devaux, M., Grace, J., Loustau, D. and Gessler, A.:  
555 Photosynthetic carbon isotope discrimination and its relationship to the carbon isotope signals  
556 of stem, soil and ecosystem respiration, *New Phytol.*, 188(2), 576–589, doi:10.1111/j.1469-  
557 8137.2010.03384.x, 2010.

558 Yamaoka, K., Nakagawa, T. and Uno, T.: Application of Akaike's information criterion (AIC)  
559 in the evaluation of linear pharmacokinetic equations, *J. Pharmacokinet. Biopharm.*, 6(2), 165–  
560 175, doi:10.1007/BF01117450, 1978.

561 Zamanian, K., Pustovoytov, K. and Kuzyakov, Y.: Pedogenic carbonates: Forms and formation  
562 processes, *Earth-Science Rev.*, 157, 1–17, doi:10.1016/J.EARSCIREV.2016.03.003, 2016.

563

- 1 Table 1. Correction factor models are fitted for Diff- $\delta^{13}\text{C}$ , DF (Degrees of Freedom), AIC<sub>c</sub>
- 2 (Akaike information criterion) and [CO<sub>2</sub>] CO<sub>2</sub> concentration in ppm

<b>Model Fit</b>	<b>Equation</b>	<b>R<sup>2</sup></b>	<b>AIC<sub>c</sub></b>	<b>DF</b>
<b>Exponential</b>	$Diff - \delta^{13}C = a * (b - \exp(-c * [CO_2]))$	<b>0.99</b>	<b>-294.6</b>	<b>54</b>
<b>Polynomial</b>	$Diff - \delta^{13}C = a + b * [CO_2] + c/[CO_2]^2$	<b>0.98</b>	<b>-27.56</b>	<b>54</b>
<b>Logarithmic</b>	$Diff - \delta^{13}C = a + b * \ln([CO_2])$	<b>0.89</b>	<b>91.68</b>	<b>55</b>
<b>Lowess</b>	-----	<b>0.99</b>	<b>-170.24</b>	<b>54</b>

3 Table 2. Correction factor models are fitted for Diff- $\delta^{18}\text{O}$ , DF (Degrees of Freedom), AIC<sub>c</sub> (Akaike information criterion) and [CO<sub>2</sub>] CO<sub>2</sub> concentration in ppm.

Model Fit	Equation	R <sup>2</sup>	AIC <sub>c</sub>	DF
Power	$Diff - \delta^{18}\text{O} = a * (b^{[CO_2]}) * ([CO_2]^c)$	0.99	-337.04	51
Polynomial	$Diff - \delta^{18}\text{O} = (a + b * x)/(1 + c * [CO_2] + d * [CO_2]^2)$	0.98	-19.34	50
Stein-Hart	$Diff - \delta^{18}\text{O} = 1/a + (b * \ln[CO_2]) + (c * (\ln[CO_2])^3)$	0.96	29.77	51
Lowess	-----	0.78	128.66	51

Table 3. Parameter values for correction factor model fit for Diff- $\delta^{13}\text{C}$  & Diff- $\delta^{18}\text{O}$ .

Parameter	Value	Std Error	95% Confidence
$a^{13}\text{C}$	<b>31.007</b>	<b>0.2149</b>	<b>30.57 - 31.43</b>
$b^{13}\text{C}$	<b>0.713</b>	<b>0.002376</b>	<b>0.708995 - 0.718522</b>
$c^{13}\text{C}$	<b>0.000043</b>	<b>0.000000</b>	<b>0.000042 - 0.000043</b>
$a^{18}\text{O}$	<b>0.85</b>	<b>0.003</b>	<b>0.8455 - 0.8576</b>
$b^{18}\text{O}$	<b>0.99</b>	<b>0.00</b>	<b>0.999928 - 0.9999283</b>
$c^{18}\text{O}$	<b>0.477</b>	<b>0.0047</b>	<b>0.476871 - 0.478767</b>

**Figure 1**

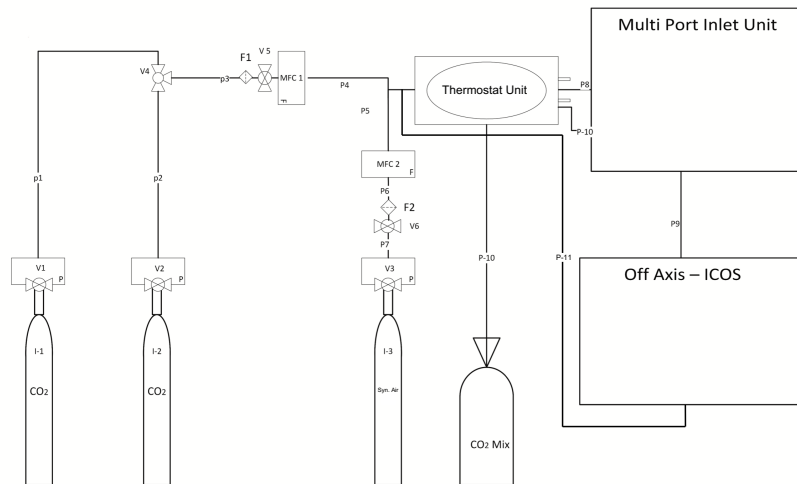


**Figure 1:** Setup made for calibration of OA- ICOS (LGR-CCIA 36-d). I(1,2): CO<sub>2</sub> standards, CO<sub>2</sub> Mix: Gas standards mixed in equal molar proportion, I3: Synthetic Air, MFC(1, 2): Mass Flow Controller, F(1, 2): PTFE filter, V(1, 2, 3): Pressure reducing Valves, V4: Three way ball valve, V(5,6): pressure controller valve with safety bypass , P (1-7): Steel pipes, P(8-11):Teflon tubing.

**Figure 2**

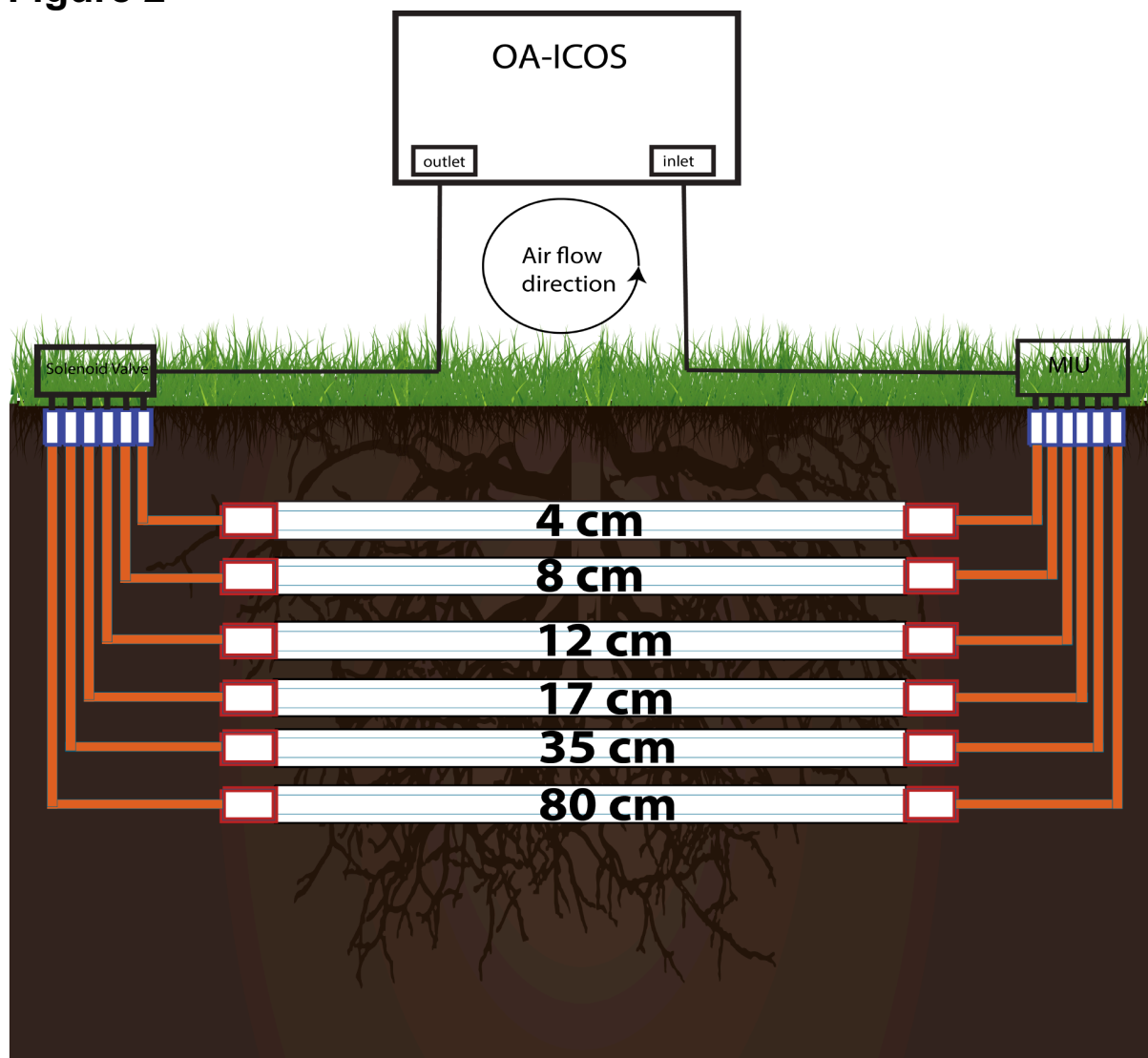


**Figure 2:** Installation made for soil air CO<sub>2</sub> [ppm],  $\delta^{13}\text{C-CO}_2$  and  $\delta^{18}\text{O-CO}_2$  measurements using an Off-Axis integrated cavity output spectrometer (OA-ICOS). Hydrophobic membrane tubing were installed horizontally in soil at different depths. MIU: multi-port inlet unit

**Figure 3**

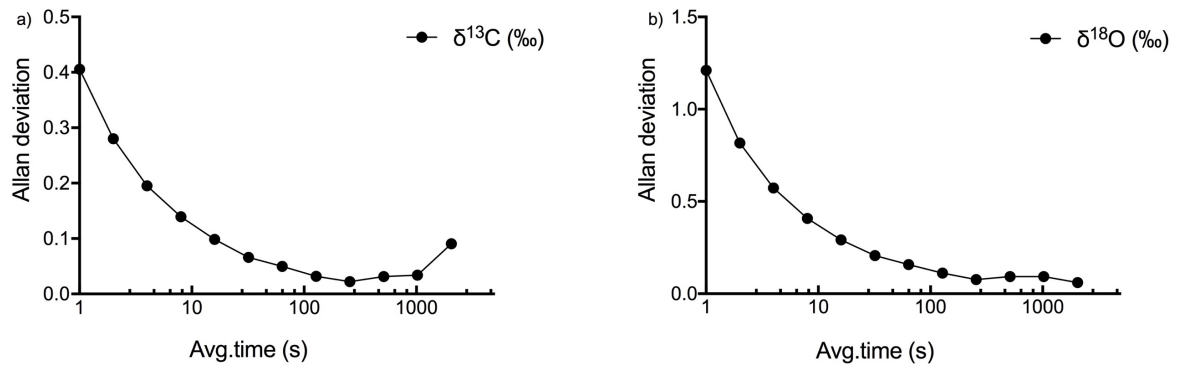


**Figure 3:** Allan deviation curve for  $\delta^{13}\text{C}$  (a) and  $\delta^{18}\text{O}$ (b) measurements by OA-ICOS CO<sub>2</sub> Carbon isotope analyzer (LGR CCIA-36d).

**Figure 4**

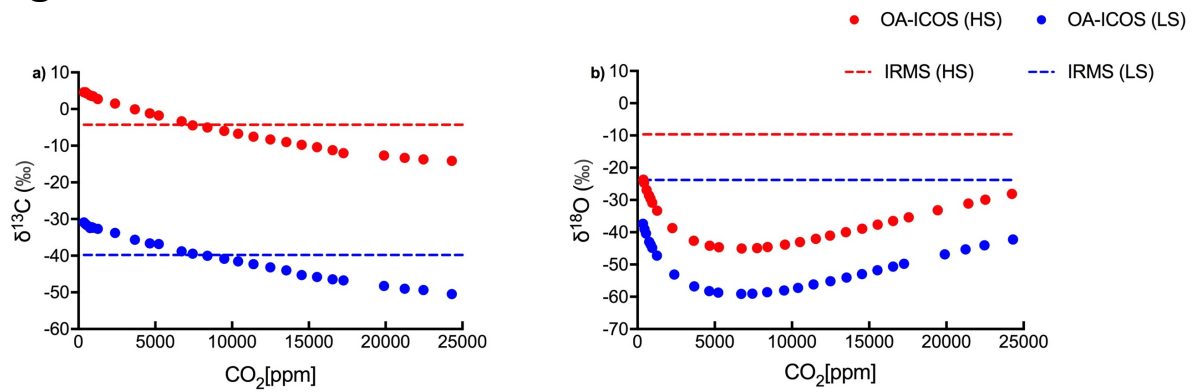


**Figure 4:** Variability observed in (a)  $\delta^{13}\text{C}$  and (b)  $\delta^{18}\text{O}$  measurements using OA-ICOS before calibration.  $\delta^{13}\text{C}$  and  $\delta^{18}\text{O}$  measured using OA-ICOS for Heavy Standard and Light Standard are shown as red and blue circles respectively. Actual  $\delta^{13}\text{C}$  and  $\delta^{18}\text{O}$  values reported after measuring by IRMS for heavy standard and light standard are shown as red and blue dashed lines respectively.

**Figure 5**

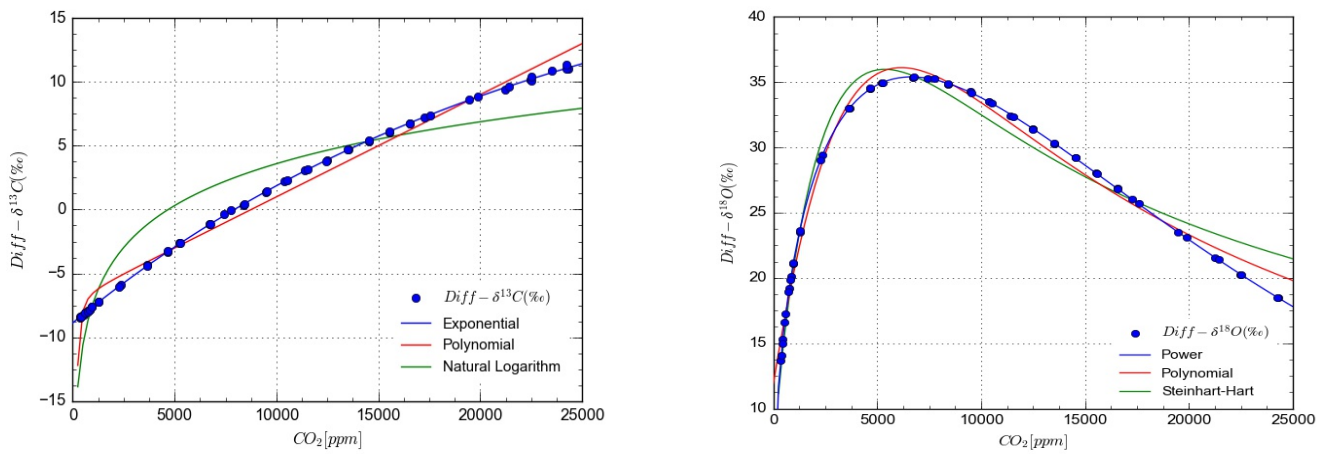


**Figure 5:** Mathematical models for concentration dependent drift in OA-ICOS measurements of stable isotopes of Carbon (a) and Oxygen (b) in CO<sub>2</sub> from IRMS measurements. Blue circles show Diff-δ<sup>13</sup>C (a) and Diff-δ<sup>18</sup>O (b) data points and lines represents different mathematical models fitted on the measured data.

**Figure 6**

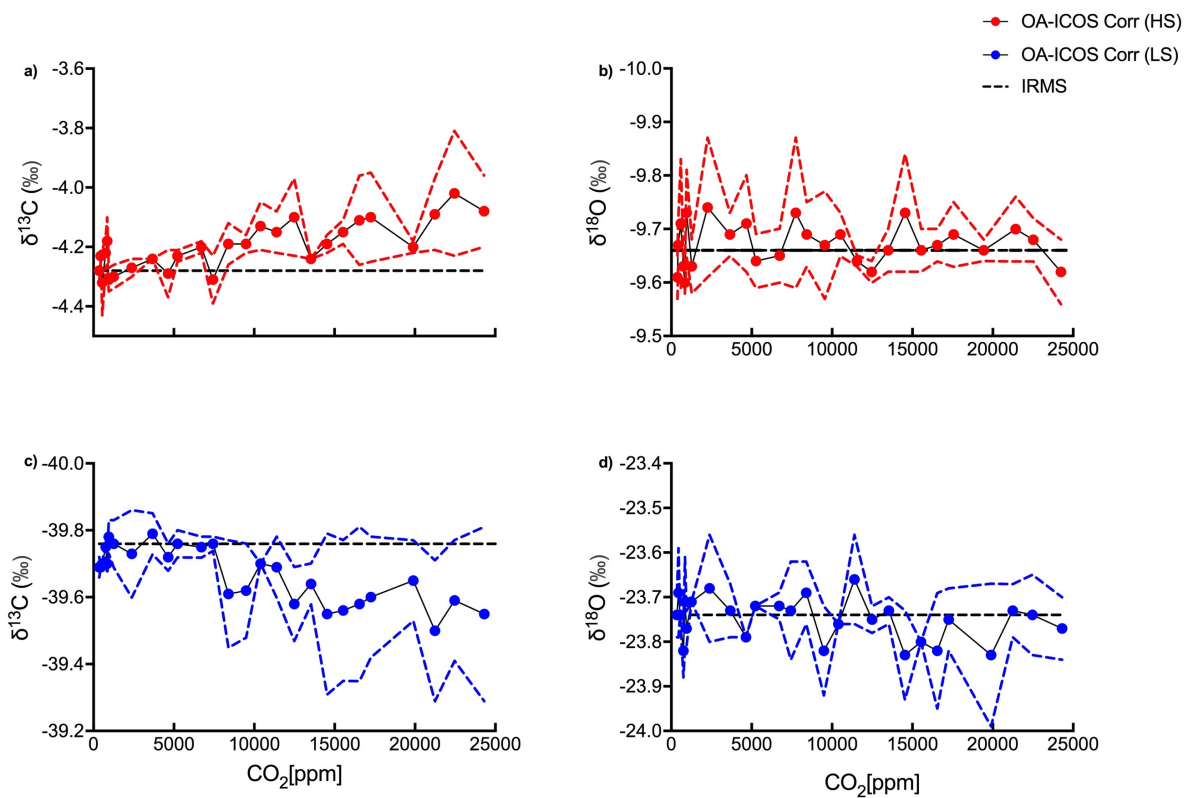


**Figure 6:** Corrected (a,c)  $\delta^{13}\text{C}$  and (b,d)  $\delta^{18}\text{O}$  measurements by OA-ICOS  $\text{CO}_2$  Carbon isotope analyzer.  $\delta^{13}\text{C}$  and  $\delta^{18}\text{O}$  measured for Heavy Standard and Light Standard are shown as red and blue circles respectively. Actual  $\delta^{13}\text{C}$  and  $\delta^{18}\text{O}$  values reported after measuring by IRMS are shown as black dashed lines and 95% confidence intervals are shown as colored dashed lines respectively.

**Figure 7**

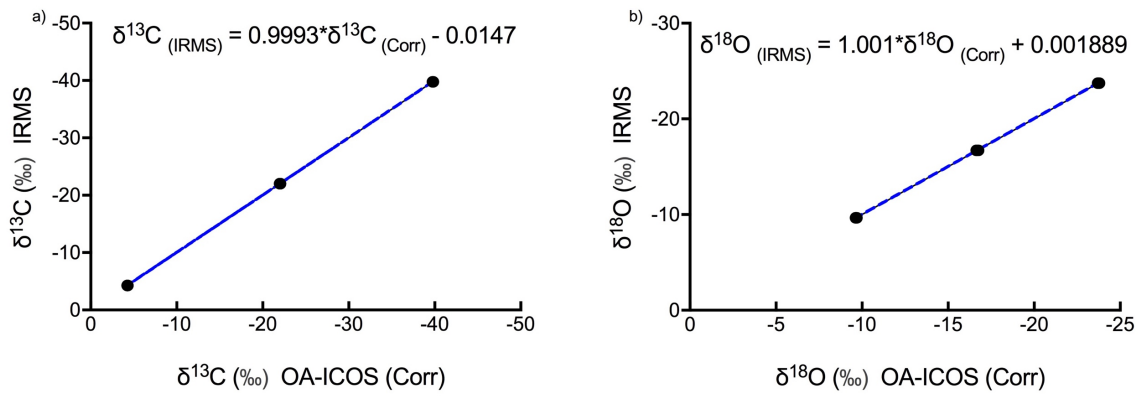


**Figure 7:** Three point Calibration lines for (a)  $\delta^{13}\text{C}$  and (b)  $\delta^{18}\text{O}$  measurements using OA-ICOS with 95% confidence interval.

**Figure 8**

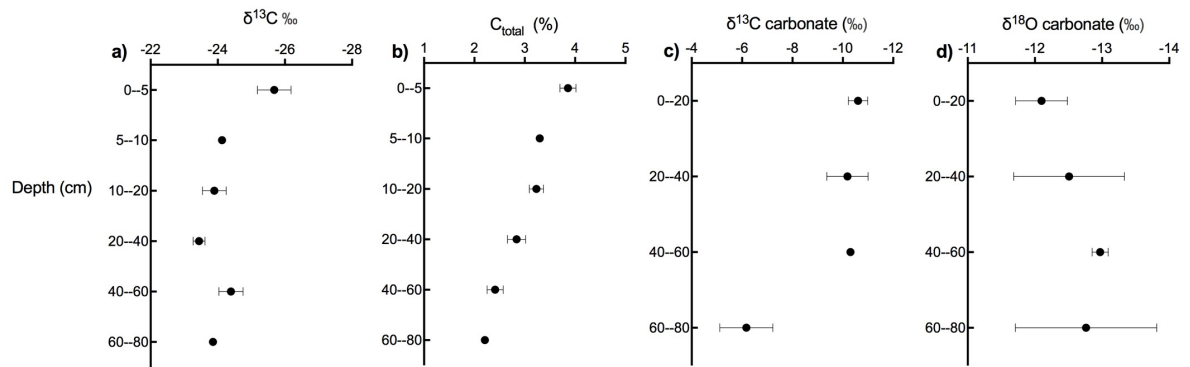


**Figure 8:** Depth profile of (a)  $\delta^{13}\text{C}$ , (b) Carbon content, (c)  $\delta^{13}\text{C}$  of soil carbonate and (d)  $\delta^{18}\text{O}$  of soil carbonate in calcareous soil.

**Figure 9**

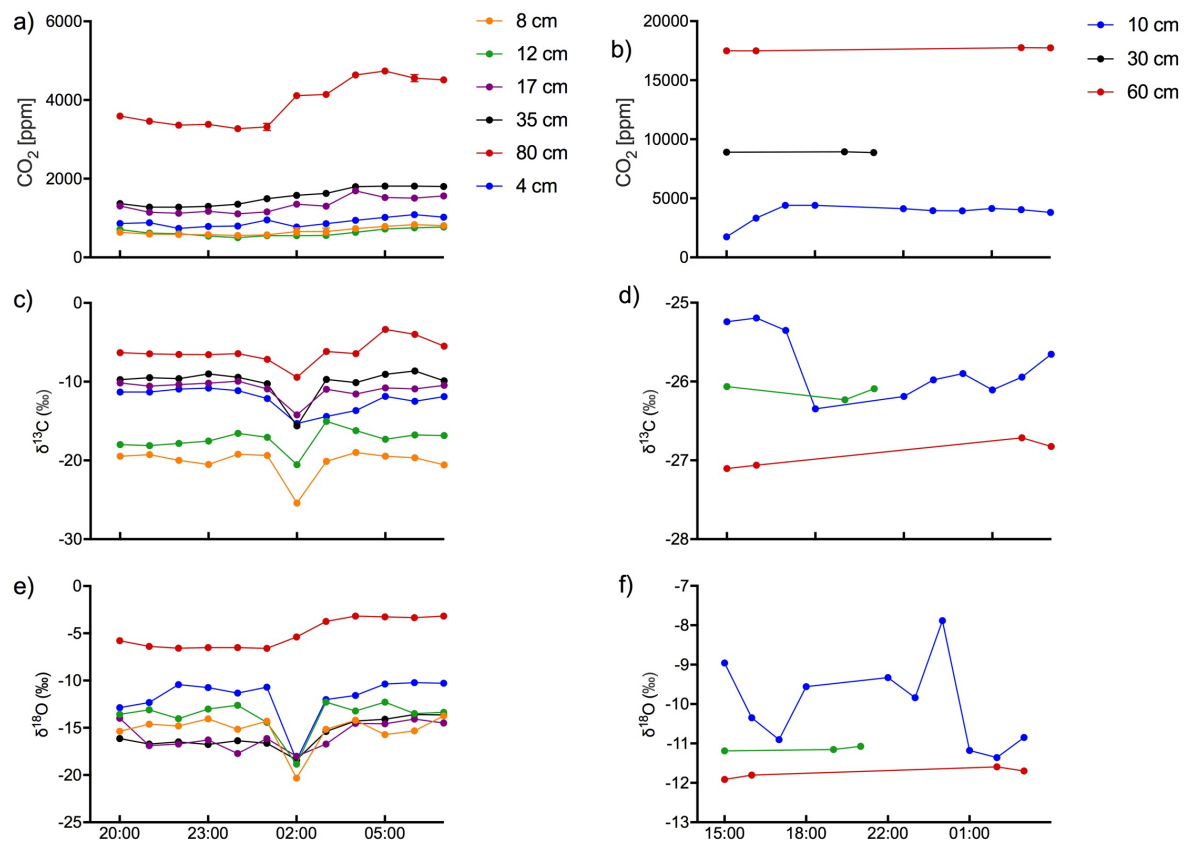


**Figure 9:** Time course of the evolution of soil gas CO<sub>2</sub> [ppm], δ<sup>13</sup>C and δ<sup>18</sup>O in calcareous (a,c,e) and acidic (b,d,f) soils. Data collected continuously over a 12 hour time frame for the calcareous soil and a 14 hour time window with intermittent data collection for the acidic soil.

**Figure 10**

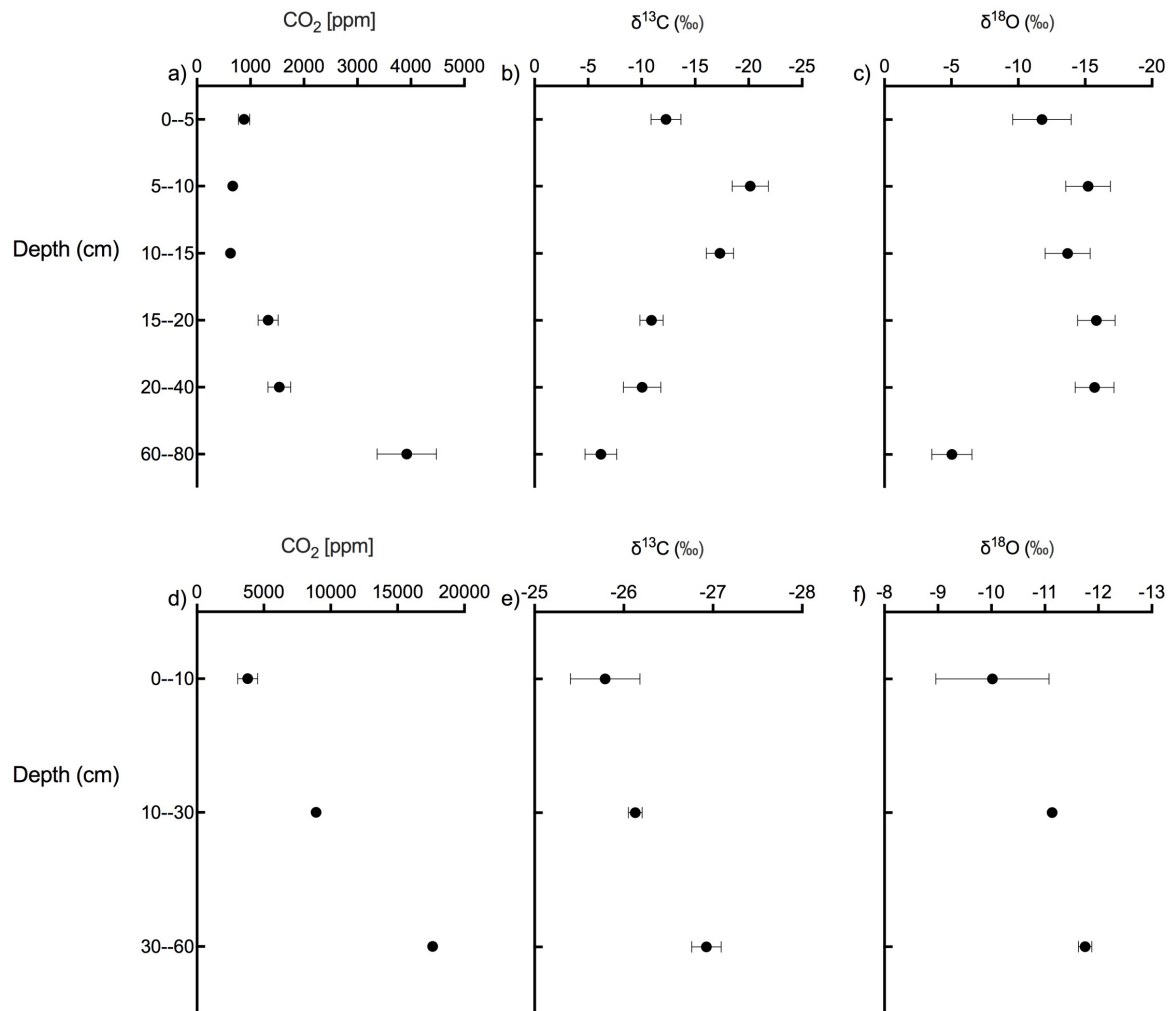


**Figure 10:** Daily average data of soil  $CO_2$  [ppm],  $\delta^{13}C$  and  $\delta^{18}O$  in calcareous (a,b,c) and acidic (d,e,f) soils across soil depth profiles.